THE JOURNAL
OF
CHEMICAL PHYSICS

VOLUME 9 OCTOBER, 1941 NUMBER 10

The Spreading of Oils on Water

Part II. Non-Ionized Molecules Having Only One Polar Group

W. A. ZISMAN
U. S. Naval Research Laboratory, Anacostia Station, Washington, D. C.
(Received June 30, 1941)

Experiments are described on the spreading upon water of drops of oil containing small amounts of alcohols, esters, ketones, phenols, non-ionized acids, and non-ionized amines. It is shown that such polar molecules do not cause spreading unless the molal concentration exceeds a certain value, c_0, which varies with the nature of the polar group, the chain length, the possible geometrical configurations of the molecule, and with the solubility in oil. The cause of their spreading is demonstrated to be a reversible adsorption at the oil-water interface associated with the osmotic pressure of the polar molecules dissolved in the oil. The average lifetime of adsorption of such molecules is shown to be only a small fraction of that of ionized molecules. A_0, the interfacial area per adsorbed molecule at the film pressure of 11.3 dynes per cm, is given for a considerable number of saturated and unsaturated straight- and branched-chain acids and alcohols. The observed changes of A_0 with chain length and polar group are explained on the basis of structural and kinetic considerations. Certain new spreading phenomena due to the formation of colloidal suspensions and crystalline precipitates of the polar compounds are described, and use is made of the latter to measure the solubility in oils of the various straight chain saturated acids and alcohols.

1. INTRODUCTION

IT was demonstrated in Part I[1] that open-chain fatty acids and amines having over 13 carbon atoms per molecule adsorbed completely at the oil-water interface if the *p*H of the water was adjusted to values greater than 10.5 or less than 3, respectively. Stated in another way, the lifetime of adsorption of the ionized polar molecule was found to be infinite.

The investigations here described were concerned with the spreading of oil drops containing non-ionized polar molecules. In order to obtain a theoretically acceptable interpretation, the alcohols were first observed, since in the *p*H range used (*p*H 2 to *p*H 13) no ionization could occur at the interface. This was followed by the study of the spreading due to fatty acids on acid water and fatty amines on alkaline water with the *p*H adjusted in each case practically to stop ionization at the oil-water interface. Finally, the other non-ionizable molecules were studied.

The white mineral oil used throughout the experiments of Part I was also employed here.

2. SPREADING DUE TO MONOHYDROXY ALCOHOLS

Each of the members of the open-chain saturated alcohols from hexanol (C_6) to eicosanol (C_{20}) was dissolved in the mineral oil and drops of each solution were spread on the clean surface

[1] W. A. Zisman, J. Chem. Phys. 9, 534 (1941).

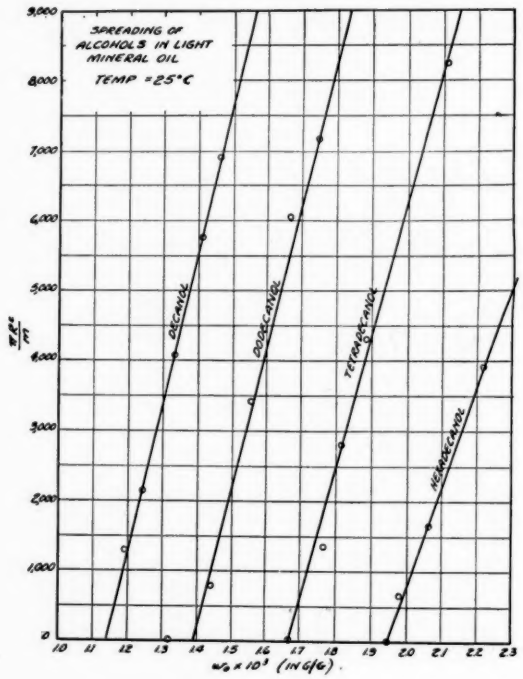

FIG. 1.

of distilled water at 25°C. It was found that spreading did not occur unless the weight concentration, w, exceeded a certain value w_0. The greater the difference $w-w_0$, the more rapid the rate of spreading and the greater the maximum area attained. For large values the films became thin enough to show uniform interference colors, in which case they broke up soon after attaining their maximum areas. The lower the molecular weight of the alcohol, the more rapid the rate of spreading, and the more violent the break-up of the oil disk. When the maximum spreading area per gram of oil ($\pi R^2/m$) was plotted against $w-w_0$, a straight line was obtained for each substance studied (see Fig. 1).

These phenomena are manifestations of short-lifetime adsorption at the oil-water interface. Every molecule of alcohol which adsorbs at the interface does not remain there indefinitely, but, due to the effects of the oil solubility of the hydrocarbon chain of the molecule and to the effects of the collisions of the interfacial molecules with one another and with the neighboring water and oil molecules, it leaves after a brief stay and disappears into the volume of the oil drop. At any instant, however, the interfacial area will contain adsorbed molecules, and their thermal agitation and mutual forces will result in the creation of a two-dimensional interfacial film pressure which will always act to increase the interfacial area. However, the spreading cannot commence until the film pressure, F, exerted by the adsorbed molecules exceeds the resultant of the surface tension forces acting on the thin oil disk. This resultant, F_0, was shown in Part I, Section 2 to be -11.3 dynes/cm for the mineral oil used.

No disk spreading can occur when w is less than w_0 because the film pressure due to the adsorbed molecules is too small. Once spreading of the oil drop can take place, the alcohol molecules adsorb as fast as new interfacial area is made available. The newly adsorbed molecules come from the alcohol distributed within the volume of the oil drop in the neighborhood of the interface, and the volume concentration in the drop decreases accordingly. Finally, the spreading ceases when the weight concentration in the drop has decreased to the value w_0, and equilibrium results. As evidence for the correctness of this description, when a multiple dropper (see Part I, Section 10) was employed to exert an external pressure on the oil drop, the disk contracted practically completely when the piston oil exerted an external pressure of only 15 dynes/cm. This is quite unlike the behavior under the same conditions of adsorbed films of ionized molecules, for they contracted only as much as necessary to obtain the closest packing of the adsorbed molecules.

Now $w-w_0$ is the amount of alcohol which had to flow from the oil drop to the interface to permit the disk to expand to its maximum spreading area S. Hence, if m is the mass of the oil drop, the number of alcohol molecules given up by the solution to form the film will be:

$$(w-w_0)m/M(6.06\times10^{23}), \qquad (1)$$

TABLE I. *Aliphatic alcohols in mineral oil (temperature 25°C).*

ALCOHOL	N	w_0 IN G/G	c_0 MOLES/1000 G	A_0 IN CM^2
Eicosanol	20	Too insoluble	—	—
Octadecanol	18	Too insoluble	—	—
Hexadecanol	16	1.94×10^{-3}	0.802×10^{-2}	57.2×10^{-16}
Tetradecanol	14	1.66×10^{-3}	0.776×10^{-2}	65.7×10^{-16}
Dodecanol	12	1.39×10^{-3}	0.749×10^{-2}	56.2×10^{-16}
Decanol	10	1.14×10^{-3}	0.722×10^{-2}	55.4×10^{-16}

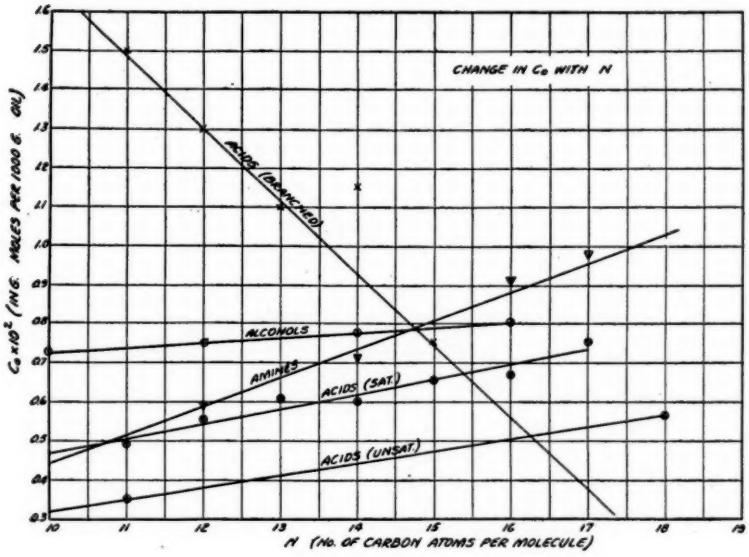

FIG. 2.

where M is the gram molecular weight of the alcohol. If A_0 is the area per interfacial molecule, and R is the maximum radius attained by the spreading oil disk, then $S=\pi R^2$, and the number of molecules in the interface must be:

$$\pi R^2/A_0. \tag{2}$$

Since expressions (1) and (2) are equal;

$$\pi R^2/A_0=(w-w_0)m/M(6.06\times10^{23}). \tag{3}$$

Differentiating (3) with respect to w gives the relation:

$$d/dw(\pi R^2/m)=A_0/M(6.06\times10^{23}). \tag{4}$$

The left-hand side of (4) is the slope, tan θ, of the straight line whose equation is given by (3), and it can be obtained by plotting $\pi R^2/m$ against w. Hence, the useful relation is obtained:

$$A_0/M=(6.06\times10^{23})\tan\theta. \tag{5}$$

This quantitative treatment may be incorrect if all of the polar material in the oil is not in true solution. If the total weight concentration of polar material added to the oil is w, it may actually consist of a colloidal portion, w_c, and a non-colloidal portion, w_s, where $w=w_c+w_s$. In measuring A_0 by diluting this solution and so measuring $\pi R^2/m$ as a function of w, the colloidal part, w_c, may vary in a complex manner depending on the history of the dilution process. Hence the quantity $(w-w_0)$ need not be the amount of polar material adsorbed at the oil-water interface at concentration w. Therefore (5) can give incorrect values of A_0 under such circumstances. This was found to be the case in studying solutions of tri-*p*-tert amylphenyl phosphate in oil.

Relation (5) does not require a precise knowledge of the state of molecular association of the polar material in solution, for so long as the value of M used is that of the unassociated molecule, the value of A_0 obtained from a spreading oil drop analysis will be the area per unassociated molecule as adsorbed at the interface. For example, if hexadecanol is studied and the value of M used in (5) is that of a single molecule, then A_0 is found to be 57.2×10^{-16} cm^2. If it is assumed that association occurs in pairs, M is twice as great and so is A_0; hence the area per chain is unchanged. Therefore no information is given as to whether or not the adsorbed molecules are also associated in pairs when adsorbed at the oil-water interface.

It was found that whereas A_0 was not temperature sensitive, w_0 was definitely so. Since w_0 is the concentration at which F equals the resultant of all the surface tension forces acting on the rim of a flat disk of oil, and since the surface tensions of oil and water are affected markedly by temperature changes, w_0 would be expected to be temperature sensitive. In fact the value of w_0 for the long-chain alcohols was found to increase roughly 5 percent for a rise of 1°C.

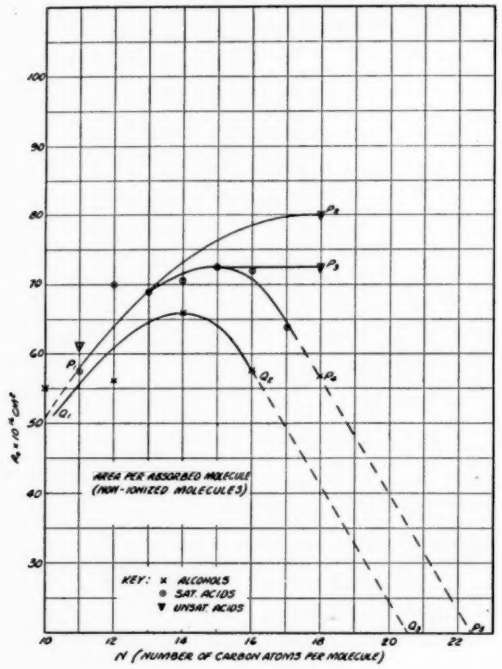

FIG. 3.

This change may be due in part to the increase with temperature of the solubility of the alcohol in oil.

The results obtained with the aliphatic alcohols are given in Table I and Fig. 1. In the third column w_0 is expressed in grams of alcohol per gram of oil, while in the fourth column c_0 is its value when expressed in gram molecules per 1000 grams of oil. In the fifth column is given, A_0, the area per adsorbed molecule.

One regularity shown by these data has been brought out in Fig. 2. Upon plotting c_0 against N, the number of carbon atoms per molecule, it is found that c_0 is a linear function of N.

Edge loss, or the edge diffusion phenomenon described in Part I, Section 4, also occurred here during and after the spreading of the oil disk. This effect became more pronounced the shorter the chain length of the molecule. The break-up effects were quite characteristic of the chain length and concentration of the polar molecules.

From the relation (5) a value of A_0 can be computed; however, the existence of edge diffusion obviously may cause the calculated value to be too small, the error being greater the more rapid the rate of edge loss, or in other words, the lower the molecular weight. That the value of A_0 is nearly correct for all values of N of Table I will later be demonstrated by an independent method of measuring A_0. In Fig. 3 will be found a plot of A_0 against N.

It might be thought that the lower values of A_0 when N decreases beyond 14 are due to the increased solubility in the water of the interfacially adsorbed molecules. Adams' well-known rule[2] that monolayers of alcohols and acids at the air-water interface are insoluble if N exceeds 12 is not true for monolayers at the oil-water interface. This is to be expected since at the latter interface the polar molecule is attracted by both the water and the oil. To prove this point a very simple experiment was performed using octanol dissolved in oil at a concentration which did not cause spreading but did show a high rate of edge diffusion. When the boundary of the disk was compressed externally with an insoluble long-chain monolayer like eicosanol, or with a film of talc, it stopped the edge diffusion. After an hour the pressure was released and the edge diffusion commenced with undiminished intensity. If the octanol molecules adsorbed at the oil-water interface had been appreciably water soluble, all of them would have been dissolved in that time since an hour is much more than the time needed for all the octanol molecules to diffuse from the oil to the interface, adsorb, and finally dissolve in the water. On the other hand a monolayer of octanol adsorbed at the air-water interface dissolved in a few minutes.

Experiments were made with mineral oil to which progressively larger amounts of hexadecanol were added until w exceeded the solubility limit as evidenced by the subsequent precipitation of crystals. It was found that as long as the solubility limit was not exceeded uniformly colored films were obtained and the graph

TABLE II. *Solubilities of alcohols in mineral oil (temperature 25°C).*

ALCOHOL	N	IN SONNEBORN PETROLATUM	IN SQUIBB'S HEAVY PETROLATUM
Octadecanol	18	Less than 2×10^{-3} g/g	Less than 2×10^{-3} g/g
Hexadecanol	16	2.5×10^{-3}	2.6×10^{-3}
Tetradecanol	14	6.1×10^{-3}	4.4×10^{-3}
Dodecanol	12	10.2×10^{-3}	8.8×10^{-3}

[2] N. K. Adam, *The Physics and Chemistry of Surfaces* (Clarendon Press, Oxford, 1938), second edition.

of $\pi R^2/m$ *versus* w was a good straight line. When w exceeded the value $w_m = 2.5 \times 10^{-3}$ gram per gram, the graph was still a straight line, but numerous colored spots appeared in the oil film during the spreading. Experiments with tetradecanol furnished similar results when w exceeded the value of $w_m = 6.1 \times 10^{-3}$, and the colored spots spread more rapidly relative to the rest of the film. A similar experiment with dodecanol resulted in $w_m = 10.2 \times 10^{-3}$, but the incidence of the phenomenon was not as sharply defined as in the case of the other two alcohols.

Since experiments showed that precipitation of crystals occurred only when the hexadecanol concentration exceeded 2.5×10^{-3}, it was concluded that w_m which was defined by the incidence of spots was actually the solubility limit. The resulting solubilities are in agreement with the well-known fact that the solubility of long chain alcohols in oil increases as the number of carbon atoms (N) decreases.

The appearance of these spots is due to the more rapid spreading of the oil disk in the vicinity of an undissolved crystal or of an undissolved droplet of the alcohol which has migrated to the oil-water interface under the influence of gravity. This change in the character of the spreading of oil drops in passing through the solubility limit can be used as a technique to measure the solubility of any slightly soluble polar substance which by itself is able to spread on water as a monolayer. However, it cannot be employed with much success if the solubility limit (w_m) is great, since the rate of disk spreading increases with the difference $w - w_0$, so that before w has reached the value w_m, the speed of spreading will have become so great that it will be impossible to differentiate with the naked eye between the spreading in the locality of the undissolved crystal and that of the surrounding film. In Table II are listed the solubilities of the three alcohols studied expressed in grams of alcohol per gram of oil. These measurements are probably correct to within ± 3 percent. Such accuracy was considered sufficient for the purpose of this work. A graph of the solubility, w_m, *versus* N is linear for Sonneborn light petrolatum, but is not for Squibb's heavy petrolatum.

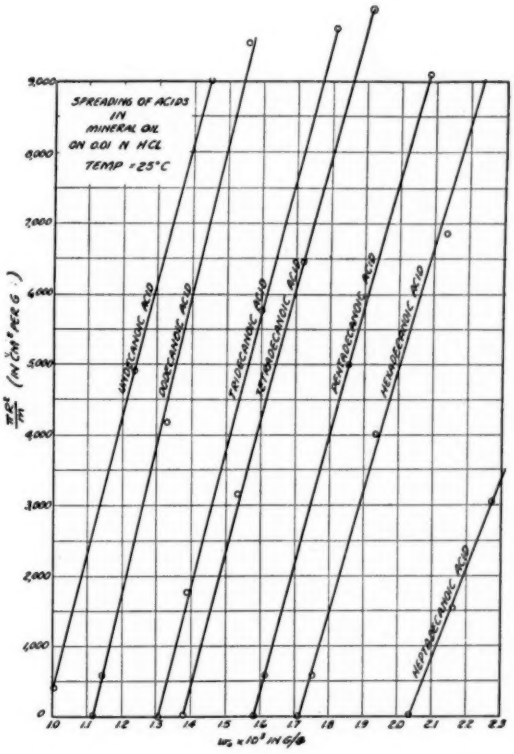

FIG. 4.

The solubility data of the preceding paragraph permit an important experimental conclusion with regard to the mechanism involved in the spreading of non-ionized molecules. If the linear increase in the area of the spreading disk with increasing w were due to the fact that the intercept w_0 was actually the solubility limit and $w - w_0$ the excess undissolved alcohol, which in that way was made available to be adsorbed and cause spreading, then necessarily the solubility limit would have to be greater for hexadecanol than for dodecanol, since from Table I w_0 increases with N. However, the solubility measurements of the preceding paragraph show that the reverse is actually the case. Hence w_0 cannot be the solubility limit, but is less than that, and the

TABLE III. *Cyclic alcohols in mineral oil (temperature 25°C).*

ALCOHOL	N	w_0	c_0
Benzyl alcohol	7	3.4×10^{-3}	3.2×10^{-2}
Diphenyl carbinol	13	0.9×10^{-3}	0.55×10^{-2}
Phenyl benzyl carbinol	14	1.0×10^{-3}	0.51×10^{-2}
Cyclohexanol	6	2.4×10^{-3}	2.4×10^{-2}
1-Ethyl cyclohexanol	8	2.7×10^{-3}	2.1×10^{-2}

difference becomes rapidly greater as N decreases (compare Tables I and II). The only conclusion left is that the spreading of oil disks containing non-ionized molecules is a manifestation of interfacial adsorption from a true solution.

The lack of disk spreading found at 25°C for eicosanol and octadecanol has a simple explanation. From Table I it is evident that w_0 increases as N increases, while from Table II the solubility, w_m, decreases as N increases. In the case of octadecanol or of homologous alcohols of still greater molecular weight, w_m is less than w_0; that is, the low solubility does not permit dissolving enough alcohol for the adsorbed molecules to exert sufficient surface pressure to cause disk spreading.

As would be expected from the fact that the alcohols do not dissociate in water, the spreading effects of alcohols in oil were found to be uninfluenced by changes in the pH of the water or by the presence of metallic ions.

The spreading effects due to cyclic alcohols were studied much more briefly and the results are given in Table III. It will be noted that c_0 is greater the greater the solubility of the alcohol in the oil. All these alcohols showed strong edge diffusion, the effect being greater the smaller the number of carbon atoms in the longest chain or branch of the molecule. In all cases the edge diffusion was too pronounced to permit accurate measurements of A_0 by observation of the maximum spreading diameters. However, w_0 could be approximately determined by seeking that concentration of alcohol in the oil which just caused the drop to begin to spread. Due to their insolubility in oil interesting alcohols like p-hydroxy diphenyl and triphenyl carbinol could not be studied.

TABLE IV-A. *Saturated acids in mineral oil—temp. 25°C (spread on 0.01 N* HCl).

ACID	N	w_0 IN G/G	c_0 MOLES/1000 G	A_0 IN CM^2
Hexacosanoic	26	Too insoluble	—	—
Eicosanoic	20	Too insoluble	—	—
Nonadecanoic	19	Too insoluble	—	—
Octadecanoic	18	Too insoluble	—	—
Heptadecanoic	17	2.05×10^{-3}	0.752×10^{-2}	63.8×10^{16}
Hexadecanoic	16	1.71×10^{-3}	0.667×10^{-2}	72.0×10^{16}
Pentadecanoic	15	1.58×10^{-3}	0.653×10^{-2}	72.6×10^{16}
Tetradecanoic	14	1.37×10^{-3}	0.601×10^{-2}	70.5×10^{16}
Tridecanoic	13	1.30×10^{-3}	0.607×10^{-2}	68.9×10^{16}
Dodecanoic	12	1.11×10^{-3}	0.556×10^{-2}	69.8×10^{16}
Undecanoic	11	0.98×10^{-3}	0.530×10^{-2}	57.4×10^{16}

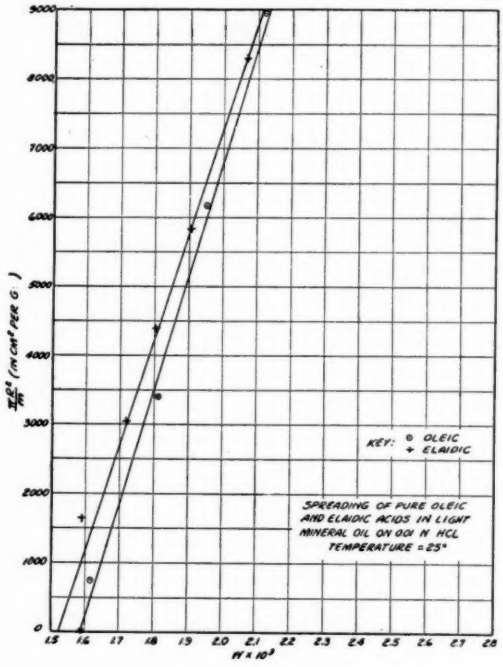

FIG. 5.

All of the alcohols described here were Eastman preparations except the 1-ethyl cyclohexanol which was kindly supplied by W. A. Mosher[3] of the Hercules Powder Company and the eicosanol which was prepared by Dr. Homer Adkins of the University of Wisconsin.

3. SPREADING DUE TO NON-IONIZED MONOCARBOXYLIC ACIDS

Each of the saturated open-chain acids described in Part I was also studied when spread on 0.01 normal HCl, and it was found in each case that precisely the same spreading phenomena occurred as have been described for the various alcohols. In Fig. 4 will be found graphs of $\pi R^2/m$ against w for these acids, while the results suitable for comparison with those for the alcohols will be found in Tables IV-A and IV-B. The eicosanoic, nonadecanoic, and pentadecanoic acids were highly purified specimens supplied by Dr. Roger Adams of the University of Illinois; the oleic and elaidic acids were freshly prepared in a high state of purity by Dr. J. Kass of the University of Minnesota. The other acids were Eastman preparations.

[3] W. A. Mosher, J. Am. Chem. Soc. **62**, 552 (1940).

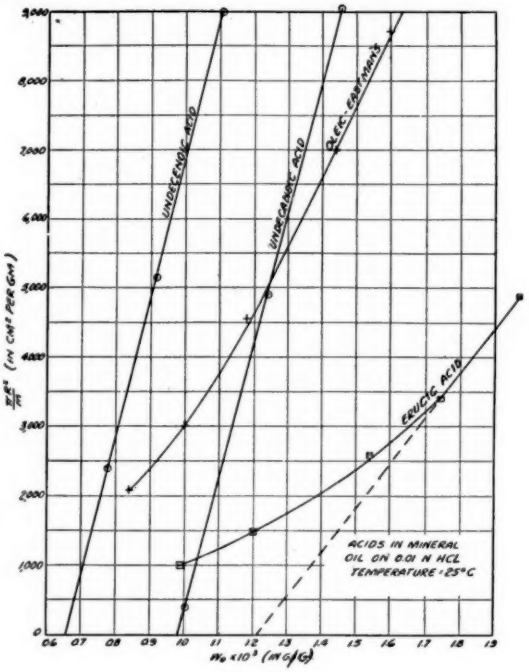

FIG. 6.

The preceding study of the spreading of alcohols furnished the clue as to the cause of the non-spreading of oil drops containing low concentrations of long-chain fatty acids on acid water (see Part I, Section 13). On acid water the fatty acids are not ionized, hence they adsorb like any other non-ionized molecules and cause disk spreading only when w exceeds a value w_0 of the order of magnitude of 10^{-3}. These conclusions evidently extend the earlier conclusion of Langmuir[4, 5] which concerned the adsorption of stearic acid at the oil-water interface. Therefore, in contrast with the behavior of ionized molecules, all non-ionized polar molecules have very short lifetimes of adsorption.

A graph of c_0 against N (see Fig. 2) is a straight line. Also the mean value of c_0 for acids is 0.613×10^{-2} while for alcohols it is 0.762×10^{-2}. The lower value for the acids can be considered either as a manifestation of the smaller solubility in oil of the acids, or more likely, as evidence of the greater energy of adhesion of the carboxyl group to water, than of the hydroxyl group.

Upon comparing the value of A_0 for each alcohol and the corresponding acid, it is evident that it is always greater for the acid. This is not due to the effect of a slight dissociation of the fatty acid at the water interface for the same results were obtained using acid water varying in strength from 0.01 to 0.05 normal.

The lower values of c_0 for the *cis-* and *trans-*isomers oleic and elaidic acids, as well as for undecenoic acid, than for the corresponding saturated acids (see Figs. 5 and 6) are noteworthy. An evident interpretation is that the presence of double bonds increases the average adsorption lifetime.

As an example of the great sensitivity of A_0 and c_0 to the state of purity of the acid preparation used, Eastman oleic acid gave a straight line graph of $\pi R^2/m$ against w only for large values of w, and from this slope the values for A_0 and c_0 were calculated to be 46×10^{-16} and 0.25×10^{-2}, respectively. In contrast the pure acid prepared by Dr. Kass gave an excellent straight line for all values of $w-w_0$, and A_0 and c_0 were calculated to be 79.8×10^{-16} and 0.564×10^{-2}, respectively (compare Figs. 5 and 6). The values of A_0 and c_0 for oleic, elaidic, and undecenoic acids when plotted in Figs. 2 and 3 led to the suggestive curves shown. From the appearance of the graph for Eastman erucic acid (see Fig. 6) it was concluded that polar impurities were present.

Just as in the case of alcohols, the saturated fatty acids showed an increasing value of c_0 as the number of carbon atoms per chain (N) increased, and similarly it was found that the solubility in the mineral oil decreased as N increased. Thus the solubility of hexacosanoic acid ($N=26$) was less than 10^{-4}, that of eicosanoic acid ($N=20$) was between 0.4×10^{-3} and 1.0×10^{-3}, that of octadecanoic acid ($N=18$) was approximately 1.0×10^{-3}, and that of tetradecanoic acid exceeded 3.0×10^{-3}.

It was found that oil drops containing octa-

TABLE IV-B. *Unsaturated acids in mineral oil—temp. 25°C (spread on 0.01 N* HCl).

ACID	N	w_0 IN G/G	c_0 MOLES/1000 G	A_0 IN CM²
Erucic	22	1.22×10^{-3}	0.361×10^{-2}	36.8×10^{-16}
Oleic	18	1.59×10^{-3}	0.564×10^{-2}	79.8×10^{-16}
Elaidic	18	1.53×10^{-3}	0.541×10^{-2}	72.7×10^{-16}
Undecenoic	11	0.650×10^{-3}	0.353×10^{-2}	61.1×10^{-16}
Linolenic	18	0.560×10^{-3}	0.202×10^{-2}	56.5×10^{-16}

[4] I. Langmuir, J. Frank. Inst. **218**, 143 (1934).
[5] I. Langmuir, Science **84**, 382 (1936).

decanoic acid did not spread on acid water at 25°C. This behavior was similar to that of octadecanol already described (Section 2) and had the same cause; i.e., w_0 for octadecanoic acid would of necessity, according to Table IV-A, be greater than for heptadecanoic acid, and therefore greater than 2.0×10^{-3}. Since the solubility of octadecanoic acid was less than 1.0×10^{-3}, disk spreading was impossible when using this mineral oil.

The results obtained with solutions in mineral oil of members of a homologous series of branched-chain acetic acid derivatives are presented in Table V. These were kindly supplied from preparations made some years ago under the direction of Dr. Roger Adams at the University of Illinois. The rapid decrease in A_0 for the last four acids was due in greater part to the rapid increase in the rate of edge diffusion as the length of the longest branched chain (N_1) decreased from 15 to 8 carbon atoms. It will be noted that c_0 is approximately a linearly decreasing function of N_1 (see Fig. 2). Due to the presence of small amounts of polar impurities, possibly formed in aging, more accurate measurements of w_0 and A_0 were not possible. As in the case of the oleic acid, already mentioned, the impurities caused sufficient departure of the $\pi R^2/m$ *vs.* w curve from linearity for low values of $w-w_0$ to make it difficult to measure accurately the intercept and slope and so obtain w_0 and A_0.

Various acid molecules containing closed hydrocarbon chains were also studied and the limits of the oil solubility are given (Table VI). The chaulmoogric and hydnocarpic acids were pure, freshly prepared specimens obtained from Dr. Roger Adams, while the other acids were Eastman chemicals. The low values of w_0 obtained for the chaulmoogric and hydnocarpic are to be attributed, at least in part, to the low oil solubilities of the hydrocarbon tails of the molecules which consist of a cyclopentyl group at the end of a saturated straight chain. Since w_m was less than w_0 it was not possible to measure A_0. As for the last three acids of this table, like the closed-chain alcohols of Table III, the edge diffusion effects were so pronounced as to prevent any accurate measurement of A_0.

TABLE V. *Aliphatic branched chain acids in mineral oil—temp. 25°C (spread on 0.01 N* HCl).

ACID	N	N_1	$w_0\times10^3$	$c_0\times10^2$	$A_0\times10^{16}$ CM²
*N-Pentadecyl acetic	0+15+2	15	2.05	0.75	63.8
Methyl N-tetradecyl acetic	1+14+2	14	(3.0–3.2)	1.15	(50–62)
Ethyl N-tridecyl acetic	2+13+2	13	2.9	1.1	55
N-propyl N-dodecyl acetic	3+12+2	12	(3.5–3.6)	1.3	(21–32)
N-butyl N-undecyl acetic	4+11+2	11	(3.9–4.2)	1.5	(15–26)
N-heptyl N-octyl acetic	7+8+2	8	4.9	1.8	13

* This is heptadecanoic acid (see Table IV-A) written for purpose of comparison as an acetic acid derivative.

A series of arylstearic acids already described in the literature[6] were kindly made available by Dr. Stirton of the Division of Industrial Farm Products Research of the Department of Agriculture. In Table VII will be found the results of measurements of w_0 and c_0 on 0.01 normal hydrochloric acid. It will be noted that c_0 does not vary considerably, the mean value being 0.23×10^{-2}. The lower values of c_0 as compared with those of the single chain molecules of Table IV-A cannot be due to the relative oil solubilities of the hydrocarbon portions of the acid molecules, for the arylstearic acids have the greater oil solubilities. It is suggested that either the lifetime of adsorption is greater for these arylstearic acids, or that they exert a greater surface pressure when adsorbed than does a monolayer containing the same number of stearic acid molecules per unit area.

4. SPREADING DUE TO NON-IONIZED AMINES

Although oil drops containing concentrations of the order of magnitude of $w=10^{-5}$ of aliphatic amines were found to spread readily on acid water and not at all on alkaline water (see Part I, Fig. 8), spreading also resulted on water of high *p*H if w exceeded a critical concentration w_0. Values of w_0 are given in Table VIII for various carefully purified primary aliphatic amines furnished generously by the chemical research laboratory of Armour and Company.

The concentration c_0 is an increasing linear function of N as shown in Fig. 2. Evidently the behavior of the aliphatic primary amines on alkaline water is entirely similar to that of the

[6] A. Stirton and R. Peterson, Ind. Eng. Chem. 32, 1137 (1940).

TABLE VI. *Various closed-chain acids in mineral oil—temp. 25°C (spread on 0.01 N HCl).*

ACID	N	w_0	c_0 MOLES/1000 G	w_m IN G/G
Chaulmoogric	18	$(1.0–1.5)\times10^{-4}$	$(0.36–0.54)\times10^{-3}$	$1.6\times10^{-4}<w_m<5.3\times10^{-4}$
Hydnocarpic	16	5.5×10^{-4}	0.22×10^{-3}	$w_m>9.5\times10^{-4}$
Dibenzyl acetic	7+7+2	1.4×10^{-4}	0.58×10^{-3}	$w_m>2.7\times10^{-3}$
Di-*n*-heptyl acetic	7+7+2	3.6×10^{-3}	1.4×10^{-2}	$w_m>6\times10^{-3}$
Cyclohexane carboxylic	7	$(1.5–1.8)\times10^{-3}$	$(1.2–1.4)\times10^{-2}$	$w_m>5\times10^{-3}$

aliphatic alcohols on water and of the aliphatic acids on acid water. In fact, so long as the polar end of the molecule cannot ionize while at the oil-water interface, all aliphatic polar molecules appear to behave analogously as regards the general character of the adsorption phenomena.

When a primary amine caused an oil drop to spread on alkaline water, it spread to a definite maximum diameter, stopped a few seconds, and then resumed spreading over a much larger area to make a thin colored film in which holes were formed during the final stages of spreading. Whereas the first stage of spreading was a characteristic effect due to the short lifetime of adsorption of undissociated amine molecules, the second stage was caused by a chemical reaction between the interfacial amine film and carbon dioxide dissolved in the water. This effect was first identified by noticing that blowing one's breath on the oil disk immediately accelerated the second stage of spreading. It was found not to be due to the air pressure, and it was concluded that the effect might be due to the carbon dioxide in the breath. Finally, when carbon dioxide vapor from a piece of "dry ice" was formed over the disk, the effect showed immediately in a most pronounced manner. When Na_2CO_3 was dissolved in the water, the secondary spreading effects were not accelerated, but when $NaHCO_3$ was dissolved in the water that type of spreading was always greatly accelerated. Therefore, it was concluded that the effect was caused by a reaction between the amine molecules adsorbed at the interface and the high HCO_3 ion concentration in the water surface resulting in the formation of a highly adsorbed carbonate of that amine.

A number of secondary and tertiary aliphatic amines were investigated in a similar fashion and the results are presented in Table IX. The higher values of w_0 for these amines as compared to the primary amines are possibly to be associated with their much greater oil solubilities. Similar experiments with various aromatic and naphthenic amines produced entirely similar results (see Table X).

Edge diffusion was found to a remarkable extent in secondary and tertiary amines. There is no doubt that in the case of the branched chain molecules the total number of carbon atoms per molecule N does not alone control the rate of edge diffusion, for there is a pronounced difference between branched chain and single chain molecules having the same value of N. This is in agreement with conclusions reached in Part I, Section 4.

5. SPREADING DUE TO ESTERS

Results of studying the spreading of solutions of esters are presented in Table XI. The effects were quite similar to those found for the other non-ionized molecules.

The tri-*p*-tert amylphenyl phosphate was a laboratory product of the Sharples Solvents Corporation and the tri-*p*-cresyl phosphate was an Eastman preparation. Both appeared to dissolve readily in the oil, but the very gradual formation of tiny holes in the otherwise stable colored oil films formed gave good evidence for concluding that some of the phosphates were present as a colloidal dispersion in the oil. The

TABLE VII. *Arylstearic acids in mineral oil—temp. 25°C (spread on 0.01 N HCl).*

ACID	MOLE WT.	w_0	c_0
Phenylundecylic	263	0.42×10^{-3}	0.17×10^{-2}
Phenylstearic	360	0.88×10^{-3}	0.24×10^{-2}
Ethylphenylstearic	388	1.05×10^{-3}	0.27×10^{-2}
Diisopropylphenylstearic	430	1.54×10^{-3}	0.35×10^{-2}
p-Chlorophenylstearic	395	0.66×10^{-3}	0.17×10^{-2}
Xylylstearic	293	1.26×10^{-3}	0.32×10^{-2}
Pseudocumylstearic	406	0.85×10^{-3}	0.21×10^{-2}
Cymylstearic	416	0.97×10^{-3}	0.23×10^{-2}
Tetrahydronaphthylstearic	416	0.87×10^{-3}	0.21×10^{-2}
Xenylstearic	441	0.48×10^{-3}	0.11×10^{-2}

tri-amyl citrate and the tri-amyl borate were semi-commercial products of the Sharples Solvents Corporation, and each showed the high rate of edge diffusion to be expected from molecules containing only short hydrocarbon chains. The other esters were Eastman preparations.

A group of arylstearic acid esters obtained from Dr. Stirton[6] was also studied. These were methyl- and phenyl-undecylate, ethylphenyl stearate, ethylxylyl stearate, methylphenoxyphenyl stearate, butylphenoxyphenyl stearate, and butylxylyl stearate. All gave values of w_0 in excess of 5×10^{-3}, which is from 5 to 10 times as great as the values for the corresponding arylstearic acids (see Table VII). This is presumably due to the shorter lifetime of adsorption of the ester group and to the much higher oil solubilities of esters than acids.

6. Spreading Due to Ketones

Oil solutions of various aliphatic and aromatic ketones gave results similar in their general nature to those already found for other non-ionized molecules, and the results are given in Table XII. The ketones, presumably due to their shorter lifetimes of adsorption and their higher solubilities in oil, had much larger values of c_0 than did any of the long-chain acids or alcohols.

The solubilities in oil were measured only for the least soluble ketones, i.e., di-undecyl ketone ($w_m=15\times10^{-3}$) and di-heptadecyl ketone ($w_m=1.5\times10^{-3}$). In the case of the latter, it was not possible to dissolve enough of the ketone in the oil to reach the value w_0, and hence no oil spreading could be obtained.

All the ketones studied are Eastman preparations excepting the di-heptadecyl ketone which was obtained from the Chemical Laboratory of Armour and Company.

Table VIII. *Aliphatic amines in mineral oil—temp. 25°C (spread on 0.01 N* NaOH).

Amine	N	w_0 in g/g	c_0 in moles/1000 g
Octadecyl amine*	18	Too insoluble	—
Heptadecyl amine	17	2.5×10^{-3}	0.98×10^{-2}
Hexadecyl amine	16	2.2×10^{-3}	0.91×10^{-2}
Tetradecyl amine	14	1.5×10^{-3}	0.71×10^{-2}
Dodecyl amine	12	1.1×10^{-3}	0.59×10^{-2}
Octadecenyl amine	18	0.91×10^{-3}	0.34×10^{-2}

* Solubility, w_m, is between 1.7×10^{-3} and 2.3×10^{-3} g/g.

7. Spreading Effects Due to Phenols and Naphthols

Adding either phenols or naphthols to oil did not cause spreading unless w exceeded a critical value w_0 which is listed in Table XIII. There was no observed effect of varying the pH of the water except at high pH (say pH 11) where it was found an increased rate of edge diffusion was occurring. The presence of metallic ions made no change in the phenomena of spreading or edge loss. These observations are not unexpected, since phenols are well known to behave as very weak acids. Oil soluble phenols of longer chain length might prove interesting but have not been obtainable.

The three chlorinated phenols listed in Table XIII are semi-commercial products of the Sharples Solvents Corporation, and as would be expected from their high oil solubilities the values of c_0 were high. The other phenols and the two naphthols were Eastman preparations.

8. Theoretical Considerations

A qualitative explanation of these adsorption phenomena at the oil-water interface can be given in terms of the kinetic concepts originated by Langmuir in developing the theory of monomolecular adsorption of gases on solids.[7]

Let ν be the rate polar molecules strike unit area of the interface, σ_0 be the actual cross-sectional area of an adsorbed molecule, α be the coefficient of accommodation, τ be the average lifetime of the adsorbed polar molecules, and n the average number of polar molecules adsorbed on unit area under equilibrium conditions, then:

$$\frac{n}{\tau}=\frac{\alpha\nu}{\sigma_0}(1-n\sigma_0). \tag{6}$$

This relation is based on the assumption that no forces exist between the adsorbed molecules. It has already been suggested here and in Part I that forces did exist between the adsorbed polar molecules and oriented hydrocarbon molecules derived from the oil resulting in the formation of a compact mixed film at the oil-water interface. In addition, evidence will be given here for concluding that cohesive forces between the

[7] I. Langmuir, J. Am. Chem. Soc. **40**, 1361 (1918).

TABLE IX. *Aliphatic secondary and tertiary amines in mineral oil—temp. 25°C (spread on 0.01 N NaOH).*

AMINE	N	w_0	c_0
Di-*n*-amylamine	5+5	$w_0 > 2.2\times10^{-3}$ g/g*	$c_0 > 1.4\times10^{-2}$
Tri-*n*-amylamine	5+5+5	$w_0 > 2.6\times10^{-3}$ g/g*	$c_0 > 1.1\times10^{-2}$
Di-octylamine	8+8	$20\times10^{-3} < w_0 < 30\times10^{-3}$	$8.3\times10^{-2} < c_0 < 12.4\times10^{-2}$
Tri-octylamine	8+8+8	$w_0 < 13.8\times10^{-3}$	$c_0 < 3.0\times10^{-2}$

* Pronounced edge loss.

hydrocarbon chains of the adjacent polar molecules become the most important forces when N exceeds 13 carbon atoms per molecule.

If the solution of polar molecules is dilute, there will apply the well-known Van't Hoff relation between osmotic pressure p, molal concentration c, and absolute temperature θ. If the density of the oil is ρ and R is the gas constant, then:

$$p = (c\rho/1000)R\theta. \tag{7}$$

From the kinetic theory of ideal gases if M is the molecular weight:

$$\nu = kp/(M\theta)^{\frac{1}{2}}. \tag{8}$$

Even in dilute solutions relation (8) may be no more than a rough approximation. However, in dilute solutions ν will certainly be proportional to p, and, although its variation with θ may be complex, it will decrease as M increases, since the viscous resistance offered by the oil to the motion of polar molecules will vary with M and with the shape of the molecule.

It has been shown here that τ is infinite if the long-chain molecule is ionized at the oil-water interface, and is a very small fraction of a second if it is not ionized. It is reasonable to assume that if there is cohesion between the adsorbed polar molecules τ will be increased, while it will be less the greater the solubility of the polar molecule in the oil, other things being equal.

A quantity of importance here is A, the average area of interface occupied by the adsorbed polar molecules. Since by definition $A = 1/n$, Eq. (6) can be written:

$$A = \sigma_0/\alpha\nu\tau + \sigma_0. \tag{9}$$

Evidently the graph of A *versus* ν is a rectangular hyperbola with a horizontal asymptote at $A = \sigma_0$. In these experiments ν was increased either by increasing the concentration c of the polar molecules in solution, or by decreasing the chain length N. Actually, for high values of ν the curve may not be hyperbolic, since under such circumstances forces between polar molecules may become important.

The decrease in c_0 with N for the saturated and unsaturated straight-chain acids (see Fig. 2) cannot be due to edge diffusion, for that would cause c_0 to increase as N decreases. The most likely cause is the increased film pressure (for a given value of surface concentration) as N decreases. This is in conformity with the rule formulated in the study of adsorption at the air-water interface, to the effect that in a homologous series, provided mutual cohesive forces between the polar molecules are not important, as N decreases the film pressure rises at constant area per molecule.

The fact that the graph of c_0 *vs.* N for acids is below that for alcohols can be attributed to a greater energy of adsorption of the non-ionized carboxyl group than the alcohol group (or a greater lifetime of adsorption). Therefore, for a given value of N a smaller molal concentration is needed to obtain the pressure F_0. The graph for the unsaturated acids is below that for the saturated acids, since, for a given value of N at the air-water interface, an unsaturated acid exerts a higher film pressure than a saturated acid at the same surface concentration. In other words, the unsaturated acids are less bound by cohesive or van der Waals forces between the hydrocarbon chains.

The acetic acid series of Table V is particularly

TABLE X. *Other amines in mineral oil—temp. 25°C (spread on 0.01 N NaOH).*

AMINE	N	w_0	c_0
Dicyclohexylamine	12	$w_0 > 3.6\times10^{-3}$*	$c_0 > 2.2\times10^{-2}$
Diphenylamine	6+6	$w_0 > 2.9\times10^{-3}$	$c_0 > 1.7\times10^{-2}$
Triphenylamine	6+6+6	$w_0 > 3.9\times10^{-3}$	$c_0 > 1.6\times10^{-2}$
Dibenzylamine	7+7	$w_0 > 1.9\times10^{-2}$*	$c_0 > 0.96\times10^{-2}$
Tribenzylamine	7+7+7	$w_0 > 6.9\times10^{-2}$*	$c_0 > 2.4\times10^{-2}$

* Pronounced edge loss.

TABLE XI. *Esters in mineral oil—temp. 25°C (spread on 0.01 N HCl).*

ESTER	N	w_0 IN G/G	c_0 MOLES/1000 G
Ethyl myristate	16	$w_0 > 15.0\times10^{-3}$	$c_0 > 5.9\times10^{-2}$
Methyl stearate	19	$w_0 > 6.0\times10^{-3}$	$c_0 > 2.0\times10^{-2}$
Ethyl stearate	20	$w_0 > 6.1\times10^{-3}$	$c_0 > 2.0\times10^{-2}$
Tri-*p*-cresyl phosphate	7+7+7	1.48×10^{-3}	0.4×10^{-2}
Tri-*p*-tert amyl-phenyl phosphate	11+11+11	$1.5\times10^{-3} < w_0 < 1.9\times10^{-3}$	$0.28\times10^{-2} < c_0 < 0.35\times10^{-2}$
Triamyl citrate	7+7+6+1	$2\times10^{-3} < w_0 < 2.5\times10^{-3}$	$5.0\times10^{-2} < c_0 < 6.2\times10^{-2}$
Triamyl borate	5+5+5	$w_0 > 7\times10^{-3}$*	$c_0 > 2.6\times10^{-2}$

* Showed strong edge loss.

interesting. From Fig. 2 it is seen that the graph of c_0 *vs.* N is a straight line with a negative slope. In plotting this graph the value of N used was the number of carbon atoms (N_1) in the longest branched chain of the molecule (see column 3 of Table V). Upon constructing models of these molecules and considering various possible configurations of each, it was found that for any given member of this series some configurations were, for geometrical reasons, less likely to permit adsorption than others. Some configurations could be described roughly as various forms of the letter Y with the carboxyl group at the base, and others were like the inverted letter V with the carboxyl group hanging from the vertex between the open legs of the letter. The number of such poorly adsorbed configurations appeared greatest for the molecule $\begin{matrix}N_1\\N_2\end{matrix}>$CHCOOH when N_1 and N_2 were nearly equal, and were least when N_1/N_2 was greatest. Therefore the greatest molal concentration of acid molecules was necessary to cause oil disk spreading for the molecules having N_1 and N_2 most nearly equal. This was in agreement with the experimental results just described.

From Fig. 3 it is seen that the graph of A_0 *vs.* N has a maximum at $N=14$ in the case of the alcohols, and at $N=15$ for the acids. Relation (9) makes it clear why the early increase of A_0 with N is due to the decrease in ν caused by the lowered speed of diffusion of the polar molecules in oil as N increases. The decrease in A_0 after N exceeds 14 is due to the increased importance of the cohesional forces between adjacent hydrocarbon chains of the polar molecules, and this significantly happens when N approaches values for which the solubility in oil becomes low. This also makes the parallel behavior of the curves of Fig. 3 for alcohols and acids readily understandable, since the mechanism essentially involves reactions between the hydrocarbon chains rather than the polar groups.

The curves P_1-P_2 and P_1-P_3 of Fig. 3 were obtained by plotting A_0 for the unsaturated acids (undecylenic, oleic and elaidic). The graphical point for the first acid coincided within the experimental error with the point for saturated acids of that chain length, while the graphical points for oleic and elaidic acids were at P_2 and P_3. Upon noting that the ordinates corresponding to points P_2, P_3, and P_4 had descending magnitudes in the order of *cis*-, *trans*-, and normal-saturated configurations for 18-carbon chains, it was concluded that the cause of these differences was in the greater tendency of the saturated chains to cohere. The *trans*-configuration would be expected to be intermediate in behavior since it is more nearly a straight chain than the *cis*-configuration. These geometrical differences are quite evident upon inspecting molecular models of these substances, and their application to the interpretation of film phenomena at the air-water interface was indicated by Adam and Jessop[8] and later by Marsden and Rideal.[9]

If the various types of polar compounds investigated here are arranged in the order of the values of c_0 (as in Table XIV), they can be placed in three groups. The same grouping is obtained if values of c_0 are arranged in their order of magnitude for polar molecules having the same value of N. It will be seen that the relative order of the three groups is the same as the relative order of the solubilities of these substances in the oil. This demonstrates the importance of the solubility in oil as a variable to

TABLE XII. *Ketones in mineral oil (temperature 25°C).*

KETONE	N	w_0 IN G/G	c_0 IN MOLES/1000 G
Methylnonyl ketone	10	12.2×10^{-3}	7.2×10^{-2}
Di-*n*-amyl ketone	10	15.1×10^{-3}	8.9×10^{-2}
Di-undecyl ketone	23	12.0×10^{-3}	3.6×10^{-2}
Di-heptadecyl ketone	35	Too insoluble	—
Di-phenyl ketone	13	13.4×10^{-3}	7.3×10^{-2}
Di-benzyl ketone	15	6.0×10^{-3}	2.9×10^{-2}
Phenylundecyl ketone	18	41.7×10^{-3}	16.0×10^{-2}

[8] N. K. Adam and G. Jessop, Proc. Roy. Soc. **A101**, 516 (1922).
[9] J. Marsden and E. Rideal, J. Chem. Soc. 1163 (1938).

be considered in the study of the oil spreading due to additive polar compounds.

A result of considerable interest is evident from an inspection of Fig. 3. All the saturated straight chain alcohols and non-ionized acids have values of A_0 ranging from 50 to 72 square angstroms, whereas the same polar molecules at the same temperatures and film pressures would occupy only 20 to 25 square angstroms at the air-water interface. One would expect A_0 to be higher in the former circumstances due to some degree of film disorganization resulting from the thermal agitation of the hydrocarbon molecules of the oil. However, at film pressures as high as 11.3 dynes/cm and in proximity to high molecular weight hydrocarbon molecules, a much closer packing would be more likely. This suggests the same conclusion given in Part I, i.e., the adsorbed polar molecules form a fairly closely packed mixed film with hydrocarbon molecules derived from the oil. Such a film can be considered a two-dimensional solution. Obviously the proportion of polar to non-polar molecules in the film will vary with c, and also with the intensity of the adhesional forces between the hydrocarbon chains of the polar molecules and of the non-polar molecules. The correctness of these conclusions will be demonstrated in Part III.

TABLE XIII. *Phenols and naphthols in mineral oil—temp. 25°C (spread on 0.01 N* HCl).

PHENOL	N	w_0 IN G/G	c_0 IN MOLES/1000 G
p-tert-amyl phenol	11	0.5×10^{-3}	0.3×10^{-2}
p-cyclohexyl phenol	12	0.5×10^{-3}	0.3×10^{-2}
2-chloro-4-tertamyl-phenol	5+6	$w_0< 8.8\times10^{-3}$	$c_0<4.4\times10^{-2}$
2, 6-dichloro-4-tert-amyl phenol	5+6	$w_0>12.5\times10^{-3}$	$c_0>5.3\times10^{-2}$
2-chloro-4, 6-di-tert-amyl phenol	5+5+6	$w_0>40.0\times10^{-3}$	$c_0>1.5\times10^{-2}$
α-Naphthol	12	1.0×10^{-3}	0.6×10^{-2}
β-Naphthol	12	1.0×10^{-3}	0.6×10^{-2}

TABLE XIV. *Effect of solubility on magnitude of* c_0.

SUBSTANCE	c_0 RANGE	GROUP	MAGNITUDE OF c_0
Chaulmoogric and hydnocarpic acids	$(0.2–0.5)10^{-3}$	I	10^{-3}
Arylstearic acids	$(0.2–0.3)10^{-2}$	II	10^{-2}
Unsaturated acids	$(0.35–0.56)10^{-2}$		
Saturated acids (Straight-chain)	$(0.5–0.75)10^{-2}$		
Saturated alcohols	$(0.72–0.80)10^{-2}$		
Straight-chain amines	$(0.6–1.0)10^{-2}$		
Esters	$(0.2–.60)10^{-1}$	III	10^{-1}
Ketones	$(0.3–1.6)10^{-1}$		

The cooperation of Dr. Roger Adams of the Department of Chemistry of the University of Illinois has been a source of encouragement, as well as the essential pure organic compounds already listed. A wealth of useful chemical information concerning hydrocarbons and polar additives was made available during the course of this work through numerous discussions with Dr. Parry Borgstrom.

Determination of Diffusion Coefficients

B. SERIN* AND R. T. ELLICKSON
Department of Physics, Polytechnic Institute of Brooklyn, Brooklyn, New York
(Received July 7, 1941)

Diffusion equations derived from Fick's law are discussed and applied to experimental data in the literature on the diffusion of oxygen in copper and on reaction rates for chemical reactions in the solid phase. Previous limitations on the applicability of the formulae are removed by the use of a simple graphical method so that the theory can be applied to data to which it was previously inapplicable. It is pointed out that the exact solution to Fick's law obtained is equivalent to the parabolic law in the early stages of the diffusion process. The activation energy for the diffusion of oxygen in copper is found to be 50.5 kcal. per g-atom.

INTRODUCTION

IN an earlier paper[1] a set of equations was derived governing diffusion in solids under various boundary conditions. It was shown, for example, that if a slab of infinite extent and thickness L, in which the concentration of a diffusing material is zero at $t=0$, is placed in a region where the concentration is maintained at a value C_0 at the boundaries of the slab, one could obtain the following expression for α, the fraction of completion of the diffusion process,

$$1-\alpha=(8/\pi^2)\sum_{n\ \text{odd}}(1/n^2)\exp(-n^2\pi^2Dt/L^2). \quad (1)$$

In this expression t is the time and D is the diffusion coefficient defined by Fick's law,

$$\nabla^2C=(1/D)(\partial C/\partial t). \quad (2)$$

Similar expressions were obtained for the case of a sphere and a cylinder, the expression for a sphere[2] being

$$1-\alpha=(6/\pi^2)\sum_{n}(1/n^2)\exp(-n^2\pi^2Dt/R^2), \quad (3)$$

where R is the radius of the sphere.

It was pointed out that because of the extremely rapid convergence of the series given above, especially in the case of the slab, one could obtain values of D, or rather D/L^2, by plotting $\log(1-\alpha)$ *vs.* t and measuring the slope of the curve at large values of t, when it approaches a straight line. This procedure is quite satisfactory in many cases but suffers from one limitation. The plot will approach a straight line when all terms in the series become negligible compared to the first term. This occurs when α reaches a value of about 0.3 for the case of a slab or about 0.7 for the case of a sphere. This means that if one is dealing with diffusion in spherical particles, the diffusion process must be more than seventy percent complete before one can use the slope of the curve mentioned above to obtain a value of D/R^2. Much of the data that might be used to check the equations does not give values of α greater than about 0.5, however, and this represents a serious limitation on this method.

It is the purpose of this paper to give a simple method for obtaining a value of D/L^2 or D/R^2 from values of α however small. In fact one value may be obtained from each experimentally determined value of α. If one writes Eq. (1) in

TABLE I. *Values of α calculated from Eqs. (1) and (3).*

	SLAB		SPHERE	
kt	α	α^2/kt	α	$[1-(1-\alpha)^{1/3}]^2/kt$
0.05	0.161	0.516	0.226	0.133
0.1	0.227	0.516	0.310	0.136
0.2	0.321	0.516	0.421	0.138
0.4	0.454	0.516	0.560	0.143
0.6	0.554	0.512	0.652	0.147
0.8	0.636	0.505	0.721	0.150
1.0	0.702	0.493	0.774	0.152
1.5	0.819	0.447	0.864	0.157
2.0	0.890	0.396	0.918	0.160
3.0	0.960	0.307	0.970	0.158
5.0	0.995	0.198	0.996	0.141

* Now at the University of Pennsylvania.

[1] R. Ellickson and R. Ward, paper presented at the April, 1941 meeting of the American Chemical Society, to appear in J. Am. Chem. Soc.

[2] An expression similar to this was evidently first obtained by Fourier to represent the mean temperature of a sphere placed in a constant temperature bath.

the form,

$$\alpha = 1 - (8/\pi^2) \sum_{n \text{ odd}} (1/n^2) \exp(-n^2 kt), \quad (4)$$

where $k = \pi^2 D/L^2$, it is clear that a value of kt uniquely determines a value of α and vice versa. It is not possible to express α as a function of kt in terms of any simple functions. It can be expressed as an indefinite integral of a theta function[3] but it is doubtful that this is of much use for calculations. However, it is very easy to calculate a table of values and plot one variable as a function of the other. The results of such a calculation from Eqs. (1) and (3) are given in Table I and the curves obtained are shown in Fig. 1. These curves represent the contribution of all terms in the series and therefore can be made as accurate as desired. Now if one takes an experimentally determined value of α, the corresponding value of kt can be read from the curve of Fig. 1. Knowing the value of t to which this value of α, and therefore kt, corresponds one can calculate $kt/t = \pi^2 D/L^2$ and therefore determine D/L^2. This procedure can be repeated for every experimentally determined value of α, and a value of D/L^2 is obtained for every experimentally determined point. The same procedure can be used for the spherical case except that the other curve is used, of course.

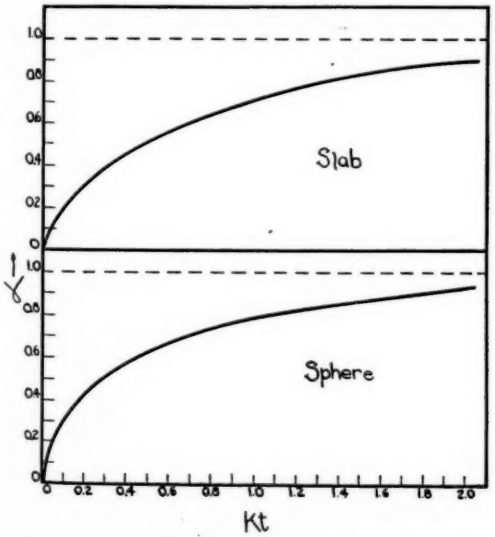

FIG. 1. α as a function of kt from Eqs. (1) and (3).

[3] Whittaker and Watson, *Modern Analysis* (Cambridge University Press, 1940), fourth edition, p. 464.

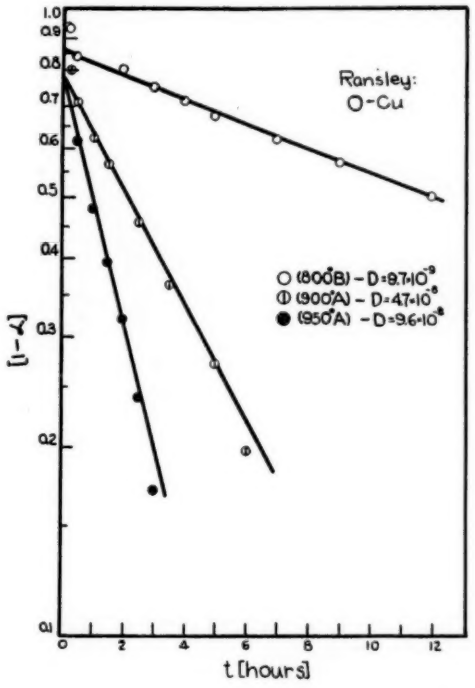

FIG. 2. Diffusion of oxygen in copper. D is expressed in cm^2 sec.$^{-1}$

DIFFUSION OF OXYGEN IN COPPER

The method described above can be applied to the data of Ransley[4] on the diffusion of oxygen in copper. These data represent the measurement of the amount of oxygen that has diffused from a strip of copper 0.09 cm thick as a function of the time. The quantity α is then the ratio of the mass of oxygen evolved at any time to the mass originally present in the strip. Some of these data were treated in our earlier paper. Figure 2 shows a plot of log $(1-\alpha)$ *vs.* t and it is observed to give a fairly good straight line at large values of t; the intercepts lie quite near the theoretical value of 0.8. However, the data taken at lower temperatures cannot be handled by that method and we shall treat it by the method described in this paper.

In Table II are given values of α, t, kt, and kt/t; the last of these should be a constant and the table shows this to be fairly true. The letters (A) and (B) indicate two different samples of copper with different initial concentrations of

[4] C. E. Ransley, J. Inst. Metals **65** (1939). (Advance copy.)

oxygen, the values being 0.41 and 0.24 percent, respectively. The fact that sample B had the lower initial concentration may account for the fact that it seems to check better with the theory. This may indicate some dependence of D on concentration, a possibility that we have not considered here. The table shows that the data agree quite well with the theory. Figure 3 shows a plot of Eq. (4) with the average value of k as obtained above. It is probably true that the agreement is within experimental error.

Ransley obtained rather good agreement with experiment using the parabolic law $\alpha^2=ct$; one might expect this since this law is derived from an assumption that is a fairly good approximation to that upon which Fick's law is based. The assumption, that the rate of diffusion through a thin strip is inversely proportional to the thickness of the strip, is an especially good approximation for small thicknesses. It is an interesting fact that the series of Eq. (1) can be quite well represented by the parabolic law in the early stages of the diffusion process. Table I shows that the parabolic law is equivalent to the exact solution

TABLE II. *Data on diffusion of oxygen in copper.*

t (HR.)	α	COPPER-OXYGEN kt	kt/t
		600°C (A)	
62.5	0.077	0.0115	1.84×10^{-4}
110.0	0.097	0.0187	1.70
205.0	0.131	0.0331	1.61
		700°C (A)	
2.0	0.0547	0.0051	2.55×10^{-3}
4.5	0.0824	0.0132	2.93
7.0	0.0960	0.0180	2.57
8.6	0.1100	0.0236	2.76
12.0	0.1164	0.0273	2.27
		800°C (A)	
0.5	0.0907	0.0156	3.12×10^{-2}
1.0	0.1300	0.0328	3.28
2.0	0.1713	0.0585	2.92
3.5	0.233	0.104	2.97
5.0	0.254	0.124	2.48
8.0	0.308	0.182	2.28
12.0	0.377	0.280	2.33
		800°C (B)	
0.25	0.075	0.011	4.40×10^{-2}
0.5	0.098	0.020	4.00
2.0	0.202	0.078	3.90
3.0	0.256	0.125	4.17
4.0	0.298	0.170	4.25
5.0	0.330	0.210	4.20
7.0	0.383	0.286	4.10
9.0	0.436	0.374	4.15
12.0	0.500	0.490	4.10

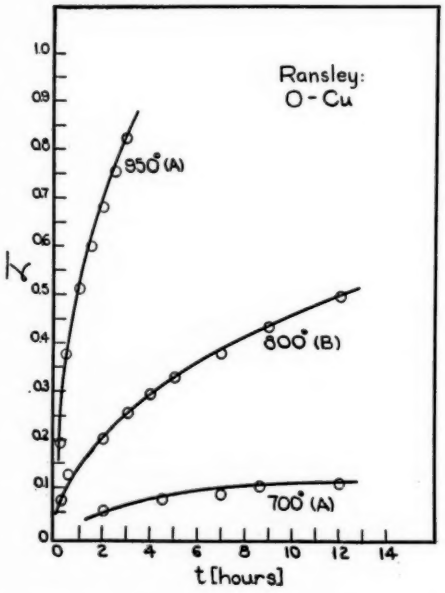

FIG. 3. Diffusion of oxygen in copper. Circles are experimental points. Solid lines are theory from Eq. (4).

within one percent for values of α up to about 0.6; for values of α greater than this the approximation becomes rapidly poorer.

The advantage in obtaining a value of the diffusion coefficient as outlined in the present paper is that the value so obtained is directly comparable with those obtained in many other diffusion experiments, especially self-diffusion,[5] where there is little doubt but that Fick's law holds.

The temperature dependence of D is given by the equation,

$$D=A\exp(-Q/RT), \tag{5}$$

where Q is the activation energy, R is the gas constant and T the absolute temperature. It is evident that a plot of log D *vs.* $1/T$ should give a straight line with slope equal to Q/R. Such a plot is shown in Fig. 4. The activation energy determined from the slope of the line is 50.5 kcal. per g-atom (2.19 ev per atom) as compared with the value of 46.0 kcal. per g-atom obtained by Ransley from a similar plot of the data treated according to his theory.

[5] F. R. Banks, Phys. Rev. **59**, 376 (1941) and references there cited.

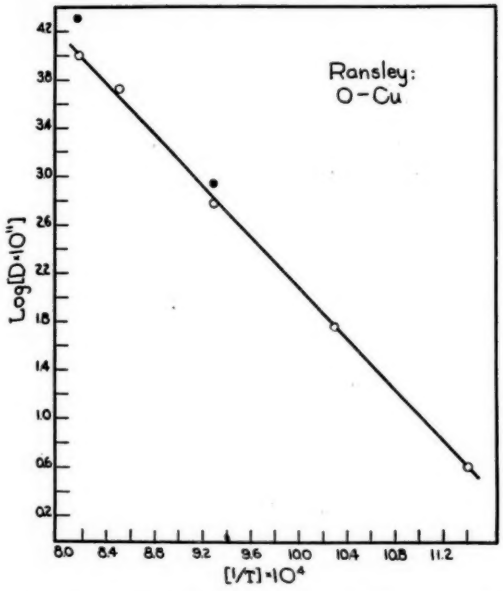

FIG. 4. Temperature dependence of diffusion coefficient of oxygen in copper. Activation energy from slope is 50.5 kcal. per g-atom.

APPLICATION TO SOLID PHASE REACTIONS

The rate of many chemical reactions that take place in the solid phase is probably governed by the rate of diffusion of one of the reactants. Assuming the particles to be spherical one can apply the theory developed here to such reactions. The data of Jander[6] on the rate of evolution of carbon dioxide in the powder reaction between barium carbonate and silicon dioxide at 830°C are given in Table III, together with values of kt and kt/t as determined from the curve of Fig. 1 for spherical particles. It is evident that the data agree with the theory remarkably well except at the very beginning of the reaction. The lack of agreement here is very probably due to the fact that there is a time lag before the entire mixture reaches a steady temperature. If one allows one minute for this time lag the agreement is excellent over the whole range. Jander estimated this time at two minutes but the correction is necessarily quite approximate. The remainder of the data on this reaction taken at various temperatures from 800°C to 890°C agrees equally well with the theory. The values of kt/t, which are proportional to D/R^2, are plotted on a logarithmic scale against $1/T$ in Fig. 5 and it may be seen that the points lie quite close to the expected straight line. The value of the activation energy (which does not depend on R) is 46.6 kcal. per mole as compared with the value of 56.0 kcal. per mole obtained by Jander.

Data from the same author on the reaction between calcium carbonate and molybdic oxide at 493°C are given in Table IV. Again it is clear that the agreement with theory is excellent. Figure 6 shows a plot of log (kt/t) *vs.* $1/T$ for this reaction at various temperatures from 487°C to 550°C. The value of the activation energy, 81.3 kcal. per mole, obtained from the slope is somewhat lower than the value of 86.3 kcal. per mole given by Jander.

Using the same assumption that leads to the parabolic law for the linear case, that material diffusing through a layer diffuses at a rate inversely proportional to the thickness of the layer, Jander derived an expression for the rate of reaction for a spherical particle,

$$[1-(1-\alpha)^{\frac{1}{3}}]^2=ct, \qquad (6)$$

where c is a constant depending on the size of the particle and the diffusion constant. The last column in Table I shows that this is not nearly as good an approximation to the exact solution based on Fick's law as is the parabolic law for the linear case.

The fraction of completion of the diffusion

TABLE III. *Rate of evolution of* CO_2 *in powder reaction.*

	$BaCO_3+SiO_2$ 830°C		
t (MIN.)	α	kt	$(kt/t)\times10^4$
3	0.021	0.0010	3.33
4	0.031	0.0015	3.75
5	0.040	0.0021	4.02
6	0.047	0.0026	4.33
7	0.054	0.0031	4.44
8	0.061	0.0039	4.87
10	0.071	0.0047	4.70
15	0.090	0.0075	5.00
20	0.100	0.0090	4.50
25	0.108	0.0106	4.24
30	0.120	0.0130	4.33
40	0.134	0.0165	4.12
50	0.146	0.0200	4.00
60	0.163	0.025	4.16
70	0.176	0.030	4.28
80	0.187	0.033	4.13
90	0.195	0.037	4.11
100	0.205	0.041	4.05
110	0.220	0.047	4.26
120	0.227	0.050	4.16

[6] W. Jander, Zeits. f. anorg. allgem. Chemie **163**, 1 (1927).

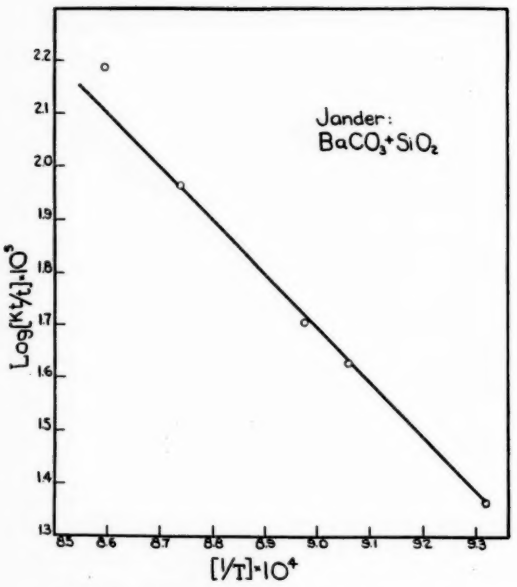

FIG. 5. Temperature dependence of reaction rate of barium carbonate and silicon dioxide. Activation energy is 46.6 kcal. per mole.

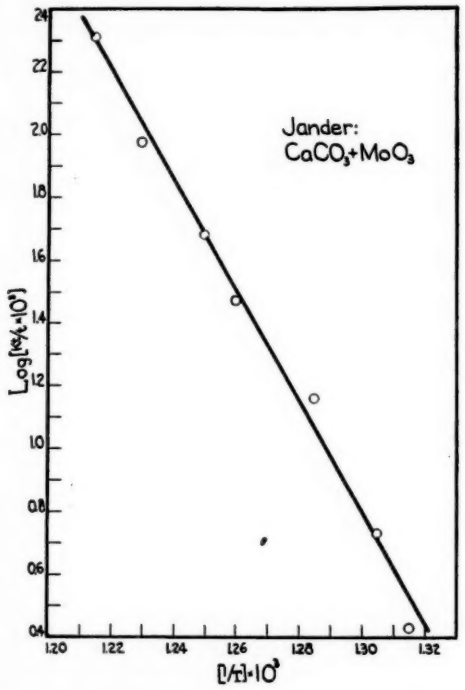

FIG. 6. Temperature dependence of reaction rate of calcium carbonate and molybdic oxide. Activation energy is 81.3 kcal. per mole.

process at any time evidently depends very strongly on the size of the particles of the diffusing substance. The value of kt/t obtained for a reaction with different sizes of particles at the same temperature should indicate to what extent the theory is valid in this regard. The value so obtained should be inversely proportional to the square of the radius of the particles used. In Table V the value of D/R^2 from Jander's data on the reaction between barium carbonate and silicon dioxide at 860°C for four different sizes of particles is given. Multiplying this value by the corresponding value of R^2 should give a constant value for D; the last column in the table shows the result to be quite satisfactory.

It should be emphasized that the method of determining D outlined in this paper is applicable only if one is dealing with particles of uniform size. If this is not the case, the solution that is valid is not that of Eq. (1) or (3) but a sum of such series, one for each size of particle. In this case the method outlined here is quite useless. One can still use the earlier method of plotting $\log(1-\alpha)$ *vs.* t and the slope of this line at large t will be proportional to D/R^2, where R is now the radius of the largest sized particles present. With a continuous distribution of particle size, the problem would be very difficult to solve, unless perhaps the distribution could be repre-

TABLE IV.

t (MIN.)	$CaCO_3+MoO_3$ 493°C α	$kt\times10^2$	$(kt/t)\times10^4$
2	0.019	0.10	5.00
3	0.030	0.15	5.00
4	0.042	0.22	5.50
5	0.050	0.29	5.80
10	0.078	0.57	5.70
15	0.093	0.80	5.33
20	0.103	1.00	5.40
30	0.125	1.43	4.77
40	0.152	2.20	5.50
50	0.171	2.8	5.60
60	0.185	3.3	5.50
70	0.198	3.8	5.43
80	0.213	4.4	5.51
90	0.226	5.0	5.65
100	0.234	5.3	5.30

TABLE V.

R (CM)	$BaCO_3+SiO_2$ 860°C D/R^2	$D\times10^{11}$ (CM² SEC.⁻¹)
0.0153	8.71×10^{-8}	2.04
0.0086	2.06×10^{-7}	1.52
0.0053	5.40×10^{-7}	1.52
0.0036	1.16×10^{-6}	1.50

sented by some very simple function. In any case, if there is more than one size of particle, the intercept will lie at a value lower than the value 0.6 predicted by Eq. (3).

In conclusion, one can say that the equations that have been developed seem to have some experimental verification. The method outlined here greatly extends the type of data that can be compared with the theory. Further experimental data, especially that covering a diffusion process carried nearly to completion, are desirable as a further check.

OCTOBER, 1941 JOURNAL OF CHEMICAL PHYSICS VOLUME 9

Thermodynamic Properties of Binary Solid Solutions on the Basis of the Nearest Neighbor Approximation

EDWIN N. LASSETTRE AND JOHN P. HOWE*
Laboratory of Chemistry, Ohio State University, Columbus, Ohio

(Received August 28, 1941)

An approximate method of computing the partition function of a binary solid solution is formulated. If the only constraints are on the mean energy and mean composition, it is shown that no metastable phase is predicted. The partition function is shown to be obtainable from the largest eigenvalue of a quadratic form and the condition for a phase transition is shown to be related to the degeneracy of the largest eigenvalue. The physical interpretation of the eigenfunction is shown to be related to the probability of surface configuration, while the square of the eigenfunction is related to the probability of a configuration on the interior of the crystal. Some simple examples are discussed which are related to the effect of coordination number on phase transitions.

THE purpose of this paper is to develop a method of calculation of the approximate partition function for a binary solid solution. It is assumed that molecules of the two components are distributed at the lattice points of a given lattice and that the energy of a configuration is determined by the interaction of nearest neighbors. The properties of this model have been studied by many investigators with the use of various approximate methods.[1] Since the critical points predicted are of considerable interest, we feel that a further investigation will be useful.

The statistical problem has been formulated by several people[2] but, to avoid confusion as to standard states, a brief presentation is included. At the same time, certain general properties of the model are obtained.

I. Formulation of Statistical Problem

For the purpose of numerical calculation, it is useful to formulate the statistical problem in terms of Gibbs's grand ensemble.[3] In terms of this scheme, the probability of finding n_1 particles of type 1 and n_2 particles of type 2 in a volume V, and state j is given by

$$\mathbf{P}(j, n_1, n_2) = \exp\left\{\frac{\Omega + n_1\chi_1 + n_2\chi_2 - E_{jn_1n_2}}{kT}\right\},$$

where $E_{jn_1n_2}$ is the energy of the jth state of a system containing n_1 particles of one kind and n_2 of the other. Ω, χ_1, χ_2 are constants to be deter-

---

* Present address, Brown University, Providence, Rhode Island.

[1] (a) W. L. Bragg and E. J. Williams, Proc. Roy. Soc. **A145**, 649 (1934); (b) H. A. Bethe, Proc. Roy. Soc. **A150**, 552 (1935); (c) J. G. Kirkwood, J. Chem. Phys. **6**, 130 (1938); (d) for a review and bibliography see F. C. Nix and W. Shockley, Rev. Mod. Phys. **10** (1938); (e) R. H. Fowler and E. A. Guggenheim, Proc. Roy. Soc. **A174**, 189 (1940); (f) H. A. Bethe and J. G. Kirkwood, J. Chem. Phys. **7**, 578 (1939); (g) J. G. Kirkwood, J. Chem. Phys. **8**, 623 (1940).

[2] The statistical problem for solutions has been presented by E. A. Guggenheim, Proc. Roy. Soc. **A135**, 181 (1932), and more recently the same author has discussed the application of the grand ensemble to the problem of regular solutions [Proc. Roy. Soc. **A169**, 134 (1938)].

[3] The principles underlying the grand ensemble are clearly presented in the book *Principles of Statistical Mechanics* by R. C. Tolman (Oxford, 1938), pp. 613–648.

mined by the conditions

$$\sum_{j,\,n_1,\,n_2} \mathbf{P}(j, n_1, n_2) = 1, \tag{1}$$

$$\sum_{j,\,n_1,\,n_2} n_1 \mathbf{P}(j, n_1, n_2) = \bar{n}_1, \tag{2}$$

$$\sum_{j,\,n_1,\,n_2} n_2 \mathbf{P}(j, n_1, n_2) = \bar{n}_2. \tag{3}$$

Here, $\bar{n}_1$ and $\bar{n}_2$ are the mean numbers of particles of each component. Ω is interpreted as $-PV$ where P is the external pressure and V is the volume of the system. χ_1 and χ_2 are the chemical potentials of components 1 and 2, respectively. The work content of the system is

$$A = -PV + \bar{n}_1\chi_1 + \bar{n}_2\chi_2.$$

In the present problem we consider a lattice consisting of M equivalent points and of such an extent that the total volume is Mv. The molecules of components 1 and 2 occupy these lattice points and a molecule of type 1 can replace a molecule of type 2 without any volume change or other distortion of the lattice.

The energy of a state depends, in general, on the composition and is assumed for our purposes to have the form

$$E_{jn_1n_2} = E_{0j} + \tfrac{1}{2}x(n_1E_1 + n_2E_2) + iV_{12},$$

where E_{0j} is the vibrational energy and depends on the size of the lattice but not on the arrangement of the particles, and E_1, E_2, and V_{12} are constants. The number of contacts between unlike molecules in a given configuration is i, and x is the coordination number of the lattice under consideration. The microscopic state of the system is then given by specifying the vibrational quantum state j, the numbers of molecules n_1 and n_2, and the positions of the molecules in the lattice. A definite arrangement of the molecules in the lattice will be called a configuration. In specifying a configuration, like molecules are to be treated as indistinguishable. An exchange of two or more like molecules does not lead to a new configuration.

As reference states the pure substances will be used so we consider the conditions (1), (2), (3) for the case $\bar{n}_1 = M$, $\bar{n}_2 = 0$. Accordingly, the left side of (3) must vanish, and since each term in the sum is positive we must have $\mathbf{P}(j, n_1, n_2) = 0$ unless $n_2 = 0$. This can be approached by giving χ_2 a large negative value. We shall confine our attention to the case for which this is exactly satisfied. The only configuration is, then, the one for which $n_2 = 0$ and hence for which $i = 0$. We thus obtain

$$[R_0]^M \exp\left[\frac{-P_1{}^0V + M\chi_1{}^0 - \tfrac{1}{2}MxE_1}{kT}\right] = 1, \tag{4}$$

where $[R_0]^M = \Sigma_j \exp(-E_{0j}/kT)$. When M is sufficiently large, R_0 will approach to a constant independent of M and in what follows we suppose that M is so large that this is the case. $P_1{}^0$ is the vapor pressure of pure component 1 and $\chi_1{}^0$ is the chemical potential of the pure component. Using (4) we find

$$xE_1/2 = \chi_1{}^0 - P_1{}^0v + kT \ln R_0, \tag{5}$$

where v is the volume per lattice point, $v = V/M$, and according to our assumption is independent of composition. In a similar way

$$xE_2/2 = \chi_2{}^0 - P_2{}^0v + kT \ln R_0. \tag{5'}$$

We now introduce the following variables

$$\alpha_1 = \exp\left\{\frac{v(P_1{}^0 - P) + \chi_1 - \chi_1{}^0}{kT}\right\},$$

$$\alpha_2 = \exp\left\{\frac{v(P_2{}^0 - P) + \chi_2 - \chi_2{}^0}{kT}\right\}, \tag{6}$$

$$\lambda = \alpha_1/\alpha_2; \quad z = \exp\{-V_{12}/kT\},$$

and Eqs. (1) and (2) become

$$\alpha_2{}^{-M} = \sum_n \sum_i \Psi(M, n, i)\lambda^n z^i \tag{7}$$

and

$$-\frac{M\lambda}{\alpha_2}\frac{\partial\alpha_2}{\partial\lambda} = \bar{n}. \tag{8}$$

$\Psi(M, n, i)$ is the number of configurations in which there are M lattice points, n molecules of type 1, and i contacts between unlike molecules. Equations (5) and (5') have been used to eliminate E_1 and E_2.

The change in work content on mixing $\bar{n}_1$ molecules of component 1 with $\bar{n}_2$ molecules of component 2 is

$$A = \bar{n}_1 kT \log \alpha_1 + \bar{n}_2 kT \log \alpha_2.$$

The condition for phase equilibrium in a heterogeneous system can be expressed in terms of α_1 and α_2. Consider, for convenience, a system

consisting of two phases, I and II, and let α_1^{I} and α_1^{II} be the values of α in the two phases. In order that the two phases be in equilibrium in the absence of external fields we must have $\alpha_1^{I}=\alpha_1^{II}$ and $\alpha_2^{I}=\alpha_2^{II}$. These functions are thus similar to but not identical with activities.

Certain useful properties of this model can be established without approximation and without complicated analysis. In the interests of clarity, these properties and the proofs are given at this point.

(a) The function α for a component increases monotonically as the mole fraction of that component increases.

We note that $(1/\lambda\alpha_2)^M$ decreases as λ increases, as is obvious from Eq. (7) when we remember that the number of configurations must be positive. Also, using Eqs. (7) and (8), we find that

$$\lambda\frac{\partial\bar{n}_1}{\partial\lambda}=(\langle n_1^2\rangle_{Av})-(\langle n_1\rangle_{Av})^2,$$

where $(\langle n_1^2\rangle_{Av})$ and $(\langle n_1\rangle_{Av})^2$ are, respectively, the average of the square and the square of the average number of molecules of type 1. The derivative of $\bar{n}_1$ with respect to λ is, therefore, positive, and hence $\bar{n}_1$ increases as λ increases. Since $\alpha_1=\alpha_2\lambda$, it follows that α_1 increases with increasing λ, and hence also with increasing $\bar{n}_1$.

(b) $\Psi(M, n, i)=\Psi(M, M-n, i)$.

Consider a configuration of n molecules of type 1 on M lattice points with i contacts. If we replace each molecule of type 1 by a molecule of type 2 and vice versa we obtain a new configuration of $M-n$ molecules of type 1. The number of contacts between unlike molecules is unchanged. By means of this process, we obtain a one to one correspondence between configurations with n molecules of type 1 and those with $M-n$ molecules of type 1, and it follows that $\Psi(M, n, i)=\Psi(M, M-n, i)$.

(c) $\alpha_2^{-1}(\lambda)=\lambda\alpha_2^{-1}(1/\lambda)$.

From Eq. (7)

$$\alpha_2^{-M}(\lambda)=\lambda^M\sum_n\sum_i\Psi(M, n, i)(1/\lambda)^{M-n}z^i$$
$$=\lambda^M\sum_n\sum_i\Psi(M, M-n, i)(1/\lambda)^{M-n}z^i.$$

Using (b), the right side of the equation is just $\lambda^M\alpha_2^{-M}(1/\lambda)$.

(d) $\bar{n}(1/\lambda)=M-\bar{n}(\lambda)$.

This can be proven directly from (8) by means of a straightforward differentiation.

(e) $\alpha_1(\bar{n})=\alpha_2(M-\bar{n})$.

This follows immediately from (b), (c), and (d), together with the fact that $\lambda\alpha_2=\alpha_1$.

As a corollary, we note that the change in work content on mixing is symmetrical around the point $\bar{n}_1=\frac{1}{2}M$. This fact has been previously pointed out by Shockley.[4] It is to be noted from (d) that when $\lambda=1$, $\bar{n}=M/2$ and hence the mean composition is determined for this special value of λ. It is also of interest that α is a monotone function of the mole fraction. This fact shows that in the present model we obtain no solution corresponding to a metastable phase unless some special constraint is imposed. It is of interest to see just how the phase separation enters in the subsequent treatment.

In order to obtain an exact value of the function α_2^{-M} it would be necessary to find the numbers $\Psi(M, n, i)$, an exceedingly difficult task which has not been attempted here. Instead, we deal with the function α_2^{-M} directly and find as a result that exact computations are possible in certain simple cases.

II. Derivation of the Difference Equations

The partition function satisfies a set of linear difference equations with constant coefficients.[5] This may be obtained in the following way.

We consider a simple cubic lattice, although the method may be extended without difficulty to any type of lattice. The cubic lattice is assumed to consist of N parallel planes, each containing m lattice points. The lattice points are occupied by n molecules of type 1 and $(mN-n)$ molecules of type 2. An arrangement of molecules in a given lattice plane will be called a distribution. In the first plane we may have any one of 2^m distributions, and we denote by $\Psi_1(N, n, i)$ the number of configurations for which the distribution in the first plane is the lth distribution. If the first plane has the lth distribution, the

[4] W. Shockley, J. Chem. Phys. **6**, 130 (1938); *ibid.* **6**, 523 (1938).

[5] This derivation follows the same general argument as that used by Fowler and Rushbrooke in treating a similar problem. Trans. Faraday Soc. **33**, 1272 (1937).

second plane must have one of 2^m distributions, say the kth. If i_l denotes the number of contacts between unlike molecules in the lth distribution and ν_{lk} the number of contacts of unlike molecules between the lth and kth (assumed adjacent), then

$$\Psi_l(N, n, i) = \sum_k \Psi_k(N-1, n-p_l, i-i_l-\nu_{lk}), \quad (9)$$

where p_l is the number of molecules of type 1 in the distribution l. The sum extends over all possible distributions in the second plane. Multiply Eq. (9) by $z^i\lambda^n$ and sum over all n and i. We thus obtain after rearranging

$$\Phi_l(N) = z^{i_l}\lambda^{p_l} \sum_k z^{\nu_{lk}}\Phi_k(N-1), \quad (10)$$

where

$$\Phi_l(N) = \sum_n \sum_i \Phi_1(N, n, i) z^i\lambda^n. \quad (11)$$

Equations (10) are a set of 2^m simultaneous linear difference equations with constant coefficients. When $\Phi_l(1)$ is given, the solution is determined uniquely by these equations.

The function $\Phi_l(1)$ is the partition function for the lth distribution in a single lattice plane. This function plays the role of an initial condition, and we may consider it as being, to some extent, arbitrary. If, for example, the first layer of molecules is formed on the surface of an adsorbing crystal, $\Phi_l(1)$ will depend on the nature of the crystal. With $\Phi_l(1)$ arbitrary, we have the problem of finding asymptotic solutions of (10) which account for the thermodynamic properties of a large lattice. It is shown in the following two sections that the solutions are obtainable if we impose certain reasonable requirements on the asymptotic forms of the partition function.

III. Reduction to Algebraic Form

The grand ensemble has the property that the entropy of a homogeneous macroscopic phase under a given set of conditions is proportional to the quantity of the phase.[3] The same is true for the energy and hence for the work content. This latter condition is satisfied provided the quantities χ_1 and χ_2 become independent of Nm as N and m become large. Thus, from Eq. (7), we see that $\Phi(N) = \Sigma_l \Phi_l(N)$ is the Nth power of a number $\mu(\mu = \alpha_2^{-m})$ as N becomes large, i.e., $\Phi(N) \sim \mu^N$. Moreover, the ratio $\Phi_l(N)/\Phi(N) = \phi_l$ is the probability of finding the lth distribution in the first lattice plane, and as the number of lattice planes becomes large this number is expected to approach a constant value independent of N. These considerations suggest that we search for solutions which have the asymptotic form

$$\Phi_l(N) \sim \phi_l \mu^N. \quad (12)$$

To find such solutions, substitute $\phi_l\mu^N$ into (10) and divide by μ^{N-1} thus obtaining

$$\mu\phi_l = z^{i_l}\lambda^{p_l} \sum_k z^{\nu_{lk}}\phi_k, \quad (13)$$

Equation (13) is a set of 2^m homogeneous linear equations in 2^m unknowns ϕ_l and the condition of compatibility is

$$\det. \, |z^{i_l}\lambda^{p_l} z^{\nu_{lk}} - \mu\delta_{lk}| = 0, \quad (14)$$

where

$$\delta_{lk} = \begin{cases} 0, & l \neq k \\ 1, & l = k \end{cases}$$

and the eigenvalues are roots of Eq. (14). Since the secular equation (14) is of degree 2^m, 2^m roots exist. We designate the rth such root by μ_r and the corresponding solution of (13) by ϕ_{lr}. In the usual way, the following orthogonality condition is found to be obeyed

$$\sum_l \phi_{lr}\phi_{ls}/z^{i_l}\lambda^{p_l} = 0 \quad \text{if } \mu_r \neq \mu_s. \quad (15)$$

In what follows, we assume that the solutions have been normalized in such a way that

$$\sum_l \phi_{lr}^2/z^{i_l}\lambda^{p_l} = 1. \quad (16)$$

Equations (13) arise when the quadratic form

$$S = \sum_l \sum_k z^{\nu_{lk}}\pi_l\pi_k \quad (17)$$

is made an extreme by varying π_l subject to the constraint

$$\sum_l \pi_l^2/z^{i_l}\lambda^{p_l} = 1. \quad (18)$$

This is obvious if we use Lagrange's method of multipliers.[6] The values of π_l which make (17) an extreme are solutions of (13), and the corresponding value of the quadratic form S is a root of (14).

[6] The general maximum and minimum properties of quadratic forms is discussed in *Methoden der Mathematischen Physik* by R. Courant and P. Hilbert (Springer, 1931), pp. 1–38.

IV. Interpretation of Solutions

There remains the problem of selecting the eigenvalue of Eq. (13) which is of physical interest. Since $\phi_l/\Sigma_l\phi_l$ gives the probability of distribution l, it must always be positive. We now show that if μ_1 is the largest root of Eq. (14), and if the root is distinct, then the corresponding solution ϕ_{l1} has the property $\phi_{l1}/\Sigma_l\phi_{l1} \geqslant 0$ and is the only solution having this property.

As previously stated, the extremes of the quadratic form S are the eigenvalues of Eq. (13). The largest eigenvalue must then be the maximum value which S can attain. Consider a set of numbers π_l which satisfy (18) and which have the property that $\pi_l > 0 (l \neq i)$, $\pi_i < 0$. The terms of S which are negative are $z^{p_l i}\pi_l\pi_i (l \neq i)$. If we vary the set by replacing π_i by $-\pi_i$ these terms become positive, and the magnitude of S increases. This variation obviously satisfies the constraint. Hence if the numbers π_l make S a maximum, π_i must have the same sign as $\pi_l (l \neq i)$. In a similar fashion, it can be shown that π_l has the same sign for all values of l. The above argument shows that the best trial set is one in which the numbers are either all positive or all negative. Hence the solution ϕ_{l1}, corresponding to the largest eigenvalue, has either the property that $\phi_{li} \geqslant 0$ (all l) or $\phi_{l1} \leqslant 0$ (all l).

Now consider any other solution ϕ_{ln}. Since the largest eigenvalue is distinct, ϕ_{ln} is orthogonal to ϕ_{l1} as in Eq. (15). This is only possible when ϕ_{ln} changes sign as l changes.

The above argument demonstrates that if we substitute any arbitrary real numbers π_l in (17) which satisfy the constraint (18), we obtain a lower bound to the eigenvalue of physical interest, i.e., $S \leqslant \mu$. This result is useful for the purpose of making approximate numerical calculations. In the future, we designate ϕ_{l1} simply by ϕ_l.

Using the fact that $\Phi(N) \sim \mu^N$ and the formula for mean composition previously given, we find that

$$\frac{N\lambda}{\mu}\frac{\partial\mu}{\partial\lambda} = \bar{n}.$$

This follows since, from (7), μ is equal to α_2^{-m}. By means of a straightforward calculation shown in the appendix, we find that

$$N\sum_l p_l\phi_l^2/z^{i_l}\lambda^{p_l} = \bar{n}. \tag{19}$$

From this formula, the mean composition can be calculated directly from the solutions to Eqs. (13).

It is interesting that Eq. (19) implies (but does not prove) that $\phi_l^2/z^{i_l}\lambda^{p_l}$ gives the probability of configuration l in a lattice plane far in the interior of the lattice. A proof of this is included in the appendix.

We have thus far discussed the case in which the largest root is distinct. When the largest root is degenerate, we have several linearly independent solutions, any linear combination of which is also a solution, and hence the surface probabilities are indeterminate. In case the roots cross, certain properties of the system will, in general, change discontinuously, since the largest root is always the one of physical interest. It seems natural then to regard the temperature at which the largest root becomes degenerate as a transition temperature.

The foregoing argument shows that a sufficient condition for a transition is that the largest root becomes degenerate. In case the transition is a phase separation and m is finite, this condition is also necessary. This follows, since the condition for phase separation is that at two mean compositions $\bar{n}_a$ and $\bar{n}_b$, the values of α for component 1 must be equal, and similarly for component 2; therefore, $\lambda_a = \lambda_b$ and $\mu_a = \mu_b$. Since $(N\lambda/\mu)(\partial\mu/\partial\lambda) = \bar{n}$, it follows that

$$\left.\frac{\partial\mu}{\partial\lambda}\right|_a \neq \left.\frac{\partial\mu}{\partial\lambda}\right|_b,$$

and the first derivative of μ with respect to λ is discontinuous. However, μ is the root of an algebraic equation with analytic coefficients, and hence $\partial\mu/\partial\lambda$ is continuous unless the largest root is degenerate. This latter statement is valid only when m is finite.

We can easily see how the composition is affected from Eq. (19). By taking linear combinations of the solutions corresponding to the degenerate roots, we obtain from (19) a *range* of compositions rather than a single composition. In other words, the activity is independent of composition over a finite range of compositions.

From the results of Section I the phase boundary must be symmetrical around mole fraction $\frac{1}{2}$ and hence $\bar{n}_b = mN - \bar{n}_a$ and $\lambda_a = \lambda_b = 1$.

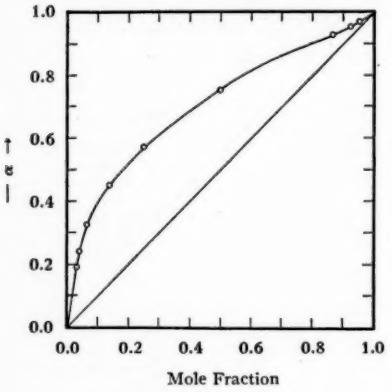

FIG. 1.

This means that a degeneracy which leads to phase separation occurs when λ is unity.[7]

On the basis of numerical calculation for special cases, the authors feel that the largest root becomes degenerate (at temperatures above absolute zero) only in the limiting case as m approaches infinity. It is true, however, that as the largest and next largest roots approach, the system tends to simulate one in which a transition is taking place.

V. Solution of Special Cases

The general Eq. (13) has not been solved in closed form, but certain special cases can be solved analytically, and these form the basis for solution by perturbation theory. Simple cases which can be treated numerically are also of interest, since they can be compared directly with the approximate calculations of other investigators.

Consider first the case of an ideal solution, i.e., one for which $z=1$. The right-hand side of Eq. (13) is then independent of l and hence if $\mu \neq 0$

$$\phi_l = A\lambda^{p_l}, \tag{12a}$$

where A is independent of l. A can be determined from the normalizing condition (16) the result being $A=(1+\lambda)^{m/2}$. If we substitute in (13) the value of μ is obtained

$$\mu = (1+\lambda)^m. \tag{13a}$$

This is the only non-vanishing eigenvalue and hence is the largest. It follows immediately from (7), and the fact that $\Phi(N) \sim \mu^N$, that $\alpha_2 = 1/1+\lambda$. From Eq. (19) we find that the mole fraction of component 1 is $X_1 = \lambda/1+\lambda$ and hence $\alpha_1 = X_1$, $\alpha_2 = X_2$. These conditions are not those ordinarily obtained for perfect solutions but are in agreement with the considerations recently advanced by Bury.[8] When the vapor pressures of the pure components are equal, these conditions reduce to Raoult's law, i.e., the activity of a given component is equal to the mole fraction of that component.

Consider next the case in which $m=1$. This corresponds to a linear lattice.[9]

The equations are

$$\begin{aligned} \mu\phi_1 &= \phi_1 + z\phi_2, \\ (\mu/\lambda)\phi_2 &= z\phi_1 + \phi_2. \end{aligned} \tag{20}$$

The roots of the secular equation are

$$2\mu = 1+\lambda \pm ((1-\lambda)^2 + 4\lambda z^2)^{\frac{1}{2}}. \tag{21}$$

These roots become equal only when $z=0$ and $\lambda=1$. When $\lambda<1$, the largest root is 1 and $\bar{n}=0$. When $\lambda>1$, $\mu=\lambda$ and $\bar{n}=N$. When $\lambda=1$, $\mu=1$ and from Eq. (19) we see that the mole fraction may vary between 0 and 1, the activity being independent of composition and equal to unity. This illustrates the behavior of the equations at a transition point.

Using Eqs. (20) and (21), α can be computed as a function of composition; the results are shown in Fig. 1 for the case $z=\frac{1}{3}$.

A valuable contribution to the theory has been made by Kirkwood,[1] who showed how to compute the coefficients in the expansion of the work content in powers of $1/kT$. In a recent paper, phase separation was discussed, and the condition for occurrence[10] in terms of our notation was found to be

$$-V_{12}/kT_c = (1-4/x)^{\frac{1}{2}} - 1. \tag{22}$$

When $T<T_c$, a separation into phases can take place. We note first that the coordination number x must be equal to or greater than 4 in order that T_c be real. It should be mentioned in this connection that other theories of order and disorder

[7] An exception to this may occur if the phase boundary curve (in the temperature-composition diagram) has a minimum at mole fraction $\frac{1}{2}$. This possibility is not rigorously excluded by the results of Section I, but it seems rather remote and is ignored in what follows.

[8] Bury, Trans. Faraday Soc. **36**, 795 (1940).

[9] A rigorous discussion, equivalent to this, has been given by Ising, Zeits. f. Physik **31**, 253 (1925).

[10] J. G. Kirkwood, J. Phys. Chem. **43**, 97 (1939).

also lead to results which are similar but not identical with this. For example, with the Bragg and Williams approximations $x \geqslant 1$, with the Bethe approximation $x \geqslant 3$, while in the recent quasichemical method of Guggenheim and Fowler[1(e)] $x \geqslant 3$. The investigation of a simple lattice of coordination number four has, therefore, a certain interest.

A simple lattice having coordination number 4 is that for which $m=3$, and the lattice planes contain three points at the corners of an equilateral triangle. In this case, there are 8 distributions of which two sets of three have equal probabilities by symmetry. We designate the distinct configurations by the scheme $\begin{matrix} & & \circ \\ \circ & \circ & \circ \end{matrix}$ (1) $\begin{matrix} \times & & \circ \\ \circ & \times & \times \end{matrix}$ (2) $\begin{matrix} \circ & & \times \\ \times & \times & \times \end{matrix}$ (3) $\begin{matrix} \times & & \times \\ \times & \times & \times \end{matrix}$ (4). The simultaneous equations are then

$$\begin{aligned}
\mu\phi_1 &= \phi_1+3z\phi_2+3z^2\phi_3+z^3\phi_4,\\
\mu\phi_2/z^2\lambda &= z\phi_1+(1+2z^2)\phi_2+(2z+z^3)\phi_3+z^2\phi_4,\\
\mu\phi_3/z^2\lambda^2 &= z^2\phi_1+(2z+z^3)\phi_2+(1+2z^2)\phi_3+z\phi_4,\\
\mu\phi_4/\lambda^3 &= z^3\phi_1+3z^2\phi_2+3z\phi_3+\phi_4.
\end{aligned}$$

We have solved these equations numerically for $z=\frac{1}{3}$ (i.e., $V_{12}/kT=+1.0986$). The results are shown in Fig. 2. It is evident from the figure that although α is not constant it changes very slowly with mole fraction around mole fraction $\frac{1}{2}$. When $\lambda=1$, the secular determinant factors into two quadratics. The roots of these quadratics are never equal for positive values of z except in the trivial case $z=0$. On this basis it seems that some property of the lattice other than coordination number must be involved in order to assure a phase separation. It is undoubtedly true that extension of Kirkwood's expansion to higher powers of V_{12}/kT will introduce other properties of the lattice than coordination number and thus distinguish between the three-filament lattice and an extended two-dimensional lattice with a coordination number of four. In fact, Kirkwood and Bethe[1(f)] have recently shown that, for lattices which are made up of two interpenetrating lattices, other properties than coordination number enter in the coefficient of (V_{12}/kT)[4,11].

The method developed here is complicated by the fact that algebraic equations of high degree must be solved. It has been our experience that the process of solution, especially near a critical point, involves elaborate analysis. This analysis appears to be inevitable, since the mathematical behavior of the thermodynamic functions is not simple in this neighborhood.

This complication is offset, in part, by the fact that the eigenfunctions have a direct physical significance and only the largest eigenvalue is necessary. It is pleasing also that the criterion for a critical point can be stated very simply in terms of degeneracy of the largest eigenvalue. Finally, the existence of a variational principle is of some assistance in correlating and refining approximate calculations. Progress toward obtaining numerical solutions has been made and will be reported in a later paper.

Appendix

I. Proof of equation for the mean number of particles, Eq. (19)

We have previously shown that

$$\mu=\sum_l \sum_k z^{p_l}\phi_l\phi_k, \tag{1a}$$

$$\sum_l \phi_l^2/z^{i_l}\lambda^{p_l}=l. \tag{2a}$$

If we differentiate each of these equations with respect to λ, we obtain, taking account of the

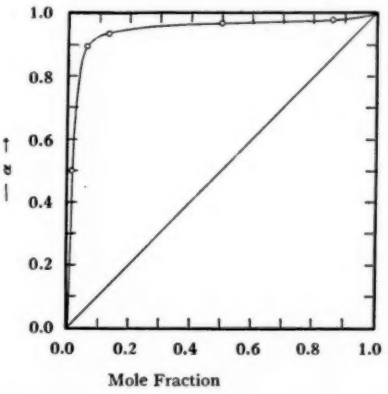

FIG. 2.

[11] As a check on the correctness of Eq. (13) we have expanded A in powers of V_{12}/kT for the case of a square plane lattice with coordination number four, and with $\lambda=1$. This was done by expanding z, μ, ϕ in powers of V_{12}/kT, the coefficients being determined by substituting in (13). The expansion coefficients thus obtained agree with those of Kirkwood and Bethe (reference 10) if we set s equal to zero in the latter and substitute the proper values of the coordination number and ζ. The fifth moment is also in agreement with that recently reported by T. S. Chang, J. Chem. Phys. **9**, 169–174 (1941).

set of simultaneous equations satisfied by ϕ_l,

$$\frac{\partial\mu}{\partial\lambda}=2\mu\sum_k\left(\phi_k\frac{\partial\phi_k}{\partial\lambda}\Big/\lambda^{p_k}z^{i_k}\right), \tag{3a}$$

$$2\lambda\sum_l\left(\phi_l\frac{\partial\phi_l}{\partial\lambda}\Big/\lambda^{p_l}z^{i_l}\right)=\sum_l\left(p_l\phi_l{}^2/\lambda^{p_l}z^{i_l}\right) \tag{4a}$$

and hence, eliminating

$$\sum_l\left(\phi_l\frac{\partial\phi_l}{\partial\lambda}\Big/\lambda^{p_l}z^{i_l}\right)$$

we get

$$\frac{\lambda}{\mu}\frac{\partial\mu}{\partial\lambda}=\sum_l\left(p_l\phi_l{}^2/\lambda^{p_l}z^{i_l}\right)=\frac{\bar{n}}{N}. \tag{5a}$$

This is Eq. (19) which we wished to prove.

II. Probability of a configuration in a lattice plane far within the interior of a lattice

Consider a lattice plane in the interior of the lattice. We suppose that there are $M-1$ planes to the left and $N-1$ planes to the right, and that the particles of the plane are arranged in accordance with the lth distribution. The partition function for the assembly is, using our previous notation and maintaining the lth distribution:

$$Q_l=\Phi_l(M)\Phi_l(N)/\lambda^{p_l}z^{i_l}. \tag{6a}$$

We divide by $z^{i_l}\lambda^{p_l}$ because, by definition, each of the functions $\Phi_l(M)$ and $\Phi_l(N)$ contains this product as a factor, and hence the numerator of (6a) contains the square of $z^{i_l}\lambda^{p_l}$. The probability of distribution l on the interior lattice plane is then

$$Q_l/\textstyle\sum_l Q_l.$$

If the lattice plane is sufficiently far in the interior of the lattice, we may replace $\Phi_l(M)$ by $\phi_l\mu^m$, $\Phi_l(N)$ by $\phi_l\mu^N$ and we obtain

$$\phi_l{}^2/\lambda^{p_l}z^{i_l} \tag{7a}$$

for the probability, taking account of the normalization of ϕ_l.

III. Asymptotic form of solution

The results of Sections III and IV may be developed in an alternative way by using an exact solution of Eq. (10). To obtain this solution we expand $\Phi_l(N)$ in a series of solutions of (13). The expansion coefficients may be obtained by substituting in (13) and using the orthogonality relations. The final result is

$$\Phi_l(N)=\textstyle\sum_r C_r\mu_r{}^N\phi_{lr}.$$

C_r is a constant (i.e., independent of N) which is obtainable from

$$C_r=\frac{1}{\mu_r}\sum_l\frac{\Phi_l(1)\phi_{lr}}{z^{i_l}\lambda^{p_l}}.$$

If μ_1 is the largest eigenvalue and is distinct

$$\Phi(N)=C_l\phi_{l1}\mu_1{}^N[1+O(\exp\{-N\log(\mu_1/\mu_r)\})].$$

It is immediately clear that when N is sufficiently large $\Phi_l(N)\sim C_l\phi_{l1}\mu_1{}^N$. Equation (12) is thus justified. In case the largest eigenvalue is degenerate, $\Phi_l(N)$ is obviously a linear combination of two or more solutions. In an actual case for which m is of order N^2 we may encounter a distribution of eigenvalues for which $\log(\mu_1/\mu_r)$ is of order $1/N$ for a range of values r. We have not been able to examine this possibility in a general way. However, in the limiting cases for which exact solutions are obtainable (i.e., at $z=0$, 1, etc.) the eigenvalues are well behaved. This fact leads us to believe that $\log(\mu_1/\mu_r)$ is not of order $1/N$ except in the neighborhood of a real transition point. In a later paper this question is investigated in some detail for one case.

The Thermal Decomposition of Methyl-*n*-Butyl Ether[1]

SIDNEY J. MAGRAM AND H. AUSTIN TAYLOR
New York University, New York, New York

(Received July 3, 1941)

The thermal decomposition of methyl-*n*-butyl ether proceeds in a manner analogous to that of the other ethers. There is no evidence to support the suggestion that it might decompose into methyl alcohol and ethylene by a ring closure through a hydrogen bond. In the first stages of the decomposition about 60 percent of the ether decomposes into CH_4 and C_3H_7CHO and about 40 percent into HCHO, C_2H_4 and C_2H_4. The decomposition of the aldehydes occurs at rates greater than that of the ether, probably induced by radicals from the ether. The butyraldehyde yields mainly CH_4, C_2H_4 and CO. First-order constants fall off as the reaction proceeds and also with diminishing pressure. The energy of activation at about 200 mm pressure is 54.0 kcal. and at 100 mm 56.6 kcal. For the reaction inhibited by nitric oxide the energy of activation is about 60 kcal.

INTRODUCTION

IN a recent paper Rice and Teller[2] have examined the question whether product molecules of a decomposition are formed in a single elementary act or through a chain mechanism, from the point of view of the principle of least motion. According to this principle the activation energy and total motion of atoms required to bring the atoms from the old to the new position should be as small as possible. On such a basis it appeared that butyl derivatives offered the possibility of forming ring structures with subsequent direct rearrangement into product molecules. Thus for methyl butyl ether, decomposition might be expected as follows:

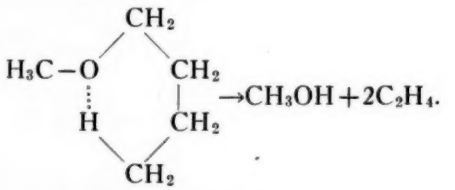

Besides presenting a difference in reaction products from those found from other ethers, the above reaction, were it to proceed, should occur at lower temperatures than those required for the chain decomposition, a simplification not to be overlooked in view of the present meager experimental data on unimolecular reactions. The occurrence of the reaction depends on the O−H "hydrogen bond" that must form. Configurationally the methyl hydrogen comes close to the oxygen atom, especially at higher temperatures when bending vibrations are excited. It appeared plausible, therefore, that at least in part the decomposition might occur by this path and determinations of the methyl alcohol produced reveal the quantitative extent of this reaction.

EXPERIMENTAL

Commercial methyl butyl ether with a boiling range of 69–72°C was fractionally distilled yielding a distillate between 70.1–70.3°C at 750 mm pressure. This was again distilled in contact with sodium and at low pressure from room temperature to −80°C using solid CO_2, several times, being finally stored over sodium at −80°C.

A liter Pyrex reaction vessel, enclosed in an electrically heated furnace, was attached to a constant volume manometer, ether storage bulbs, vacuum pumps, two Toepler pumps and a gas analysis apparatus. Since the vapor pressure of methyl butyl ether at room temperature is only about 12 cm it was necessary to heat the connecting tubing from the reaction vessel to about 50°C to prevent condensation. As a lubricant in the stopcocks which were heated, a plasticizer, di-*o*-xenylmonophenyl phosphate was found satisfactory.

In making a run, ether was allowed to vaporize into a mixing chamber surrounded by hot water to the desired pressure. In experiments with nitric oxide the latter was introduced first into

[1] Abstract from a thesis submitted by S. J. M. in partial fulfillment of the requirements for the degree of Doctor of Philosophy at New York University, February 1941.
[2] F. O. Rice and E. Teller, J. Chem. Phys. **6**, 489 (1938).

TABLE I.

TEMP. °C	P/P_i	VOL. (cc)	CO_2	CONTRACTION	O_2 CONSUMED
475	2.0	6.7	13.6	17.2	24.2
482	1.7	2.0	4.2	5.3	7.5

this chamber. The gas mixture was permitted to expand rapidly into the evacuated reaction vessel. No attempt was made to equalize the pressures. The change of pressure with time was followed for the desired period and the products were withdrawn by one of the Toepler pumps and their volume noted. The gases were then passed back and forth through a trap surrounded by an ice-toluene or liquid-nitrogen bath between the two Toepler pumps until the pressure was observed to drop to a constant value. At dry ice temperature undecomposed ether and intermediate aldehydes were condensed. All other gases, even higher possible hydrocarbons, would pass through at the pressures employed.

NORMAL DECOMPOSITION

Analytical results

The material condensed in the gas trap showed reducing properties on Tollens reagent. A fraction of a cc gave a silver precipitate from a solution of $AgNO_3$ in NH_4OH and NaOH.

One cc of the condensed material heated with 5 cc of a ten percent NaOH solution gave a yellowish brown resinous material characteristic of the lower aliphatic aldehydes. The resorcinol-sulfuric acid test showed formaldehyde present. A still more definite identification was obtained by heating a few tenths of a cc with a trace of chromotropic acid in strong sulfuric acid. A deep violet color[3] is shown by formaldehyde. Acetaldehyde, propionaldehyde and butyraldehyde do not give this test.

To establish the identity of the other aldehyde, which qualitative tests showed was present in larger amounts than formaldehyde, a derivative was made by heating a few cc of condensed material with a saturated alcoholic solution of 2.4 dinitrophenylhydrazine. This when warmed with a drop of concentrated HCl gave a yellow precipitate upon addition of water. The melting point of the compound after one crystallization from alcohol was 120–121°C. It showed no depression when mixed with the hydrazone of butyraldehyde. Since 147°C is the nearest melting point of a hydrazone, that from acetaldehyde, it is certain that the aldehyde here found is butyraldehyde.

Although many tests were made for methyl alcohol, no evidence for its presence, even in small amounts, could be found.

Analysis of the uncondensed gases showed the presence of methane, unsaturates, carbon monoxide, hydrogen and a higher hydrocarbon. The percentage of unsaturates was considerably larger than one would expect merely from analogy with the products of the lower ethers and the empirical formula of the saturated hydrocarbon mixture was considerably lower in carbon than was expected. Thus by analogy with the over-all decomposition of the lower ethers the following products might be expected:

$$CH_3OCH_2CH_2CH_2CH_3 \begin{cases} \nearrow HCHO+C_4H_{10} \rightarrow H_2+CO+C_4H_{10} \\ \searrow CH_4+C_3H_7CHO \rightarrow CH_4+C_3H_8+CO. \end{cases}$$

Only small amounts of unsaturates produced from the hydrocarbons and a total hydrocarbon content of average formula C_2H_6 is to be expected. Results show that the amounts of unsaturate are higher early in the reaction than later, that is, they constitute about 30 percent

TABLE II.

TEMP. °C	P/P_i	VOL. GAS	CO_2	CONTRACTION	O_2 CONSUMED
477	3.32	13.1	26.8	30.9	44.6
489	1.97	20.8	41.7	47.2	68.1
533	1.85	20.0	28.6	44.0	62.6
535	2.45	9.4	19.1	20.8	30.5

TABLE III.

TEMP. °C	VOL. GAS	CO_2	CONT.	O_2
477	0.49	1.00	1.15	1.67
489	.50	1.00	1.14	1.64
533	.52	1.00	1.14	1.62
535	.49	1.00	1.09	1.60
C_2H_6	.50	1.00	1.25	1.75
C_2H_4	.50	1.00	1.00	1.50

[3] F. Feigl, *Qualitative Analysis by Spot Tests.*

TABLE IV.

P/P_i	TEMP.	% CONDENSED AT −80°C	% IN KOH	C_2H_4	CO	H_2	CH_4	C_2H_6	REMARKS
1.18	480	81.1		32.8	7.1				
1.35	510	72.0		32.0	10.5	9.0	27.8	20.2	
1.41	520	69.8	1.3	31.1	14.9	9.4	27.0	16.5	287 mm ether 4.3 mm NO
1.45	496	44.1	0.3	26.1	16.4	9.5			
1.46	509	63.3		31.9	12.3				
1.70	509	53.0	0	29.3	10.4	7.0	30.0	23.5	
1.80	515	48.0	0	30.1	16.3	9.3	26.8	16.9	
1.95	496	38.0	0.3	27.5	19.9	8.1	24.2	19.8	
1.95	497		0.5	27.0	19.0				
2.00	506		1.5	30.2	18.8				large surface
2.10	500			29.0	19.2				
2.40	464	11.4	0.6	26.8	21.2	7.1	29.2	17.8	
2.40	520		0.7	25.3	22.6	6.7	29.5	14.0	287 mm ether 2.3 mm NO
2.70	519	10.6	0.6	22.1	25.3	7.6	28.7	16.3	
2.83	535	16.9	0.4	19.7	27.3	6.3	33.6	12.4	244 mm ether 0.8 mm NO
2.97	542	6.0	0.4	23.0	23.0	8.5	28.6	15.4	
3.00	551	8.8	0.3	23.2	24.1	9.0	27.3	16.2	
3.29	504		0.7	11.3	25.8	4.3	25.3	28.6	19 hours
3.30	533	8.9	0.4	18.7	27.7	7.4	30.7	15.1	1.5 hours
3.34	560		0.5	7.2	25.4	7.3	47.8	12.8	16 hours
3.35	501		0.7	8.0	26.0	3.5	26.0	36.0	30 hours
3.37	495		2.6	7.8	24.2	4.2	21.6	39.0	6 days

of the uncondensed gas so that the over-all formula of the hydrocarbon mixture is as low as $C_{1.3}H_{4.7}$.

Such a relatively high amount of unsaturate might, at first sight, suggest that the decomposition into methyl alcohol and ethylene was occurring, at least in part. The complete absence of methyl alcohol, the lowness of the percentage of unsaturates (even if the methyl alcohol were completely decomposed into CO and H_2 the ethylene percentage should still be 40), the amounts and complexity of the other products and finally the similarity of the temperature range in which methyl butyl ether decomposes to that of the lower ethers all argue against the ultimate molecule split.

To identify higher hydrocarbons they were condensed in liquid nitrogen and pumped free of H_2, CO and CH_4. Complete combustion after removal of unsaturates gave the data of Table I for the products of two runs withdrawn at the temperatures and ratios of pressure to initial pressure indicated. The ratios of the last four columns are 0.49 : 1.00 : 1.26 : 1.78 and 0.48 : 1.00 : 1.26 : 1.79 at 475° and 482°C, respectively. The ratio for C_2H_6 is 0.50 : 1.00 : 1.25 : 1.75 showing that, within the experimental error for the small volumes used, the gas is essentially ethane. It should be noted that C_3H_8 and C_4H_{10} are fairly stable at these temperatures or decompose very slowly.

The identity of the unsaturate was then obtained from a complete combustion of the unsaturate and ethane mixture. Several such results are given in Table II. In the form of ratios these data appear as in Table III. The ratio of volume of gas to CO_2 indicates that the unsaturate must be only C_2H_4. The values of contraction to oxygen consumed are consistent with mixtures of C_2H_4 and C_2H_6, though one cannot rely accurately on these values to give the ratio of C_2H_4 to C_2H_6 since, during the pumping, more C_2H_4 than C_2H_6 would be lost.

Table IV records a number of analyses at various temperatures and various stages of decomposition. The small absorption in KOH may be due to CO_2.

From these analyses and the intermediates identified it is clear that at least two simultaneous processes are occurring. One would appear to be a reaction yielding formaldehyde and hence C_4H_{10} as a residue. This residue must give C_2H_4 and C_2H_6. A radical mechanism can account for this.

$$R+CH_3OC_4H_9 \rightarrow RH+CH_2OC_4H_9,$$
$$CH_2OC_4H_9 \rightarrow HCHO+C_4H_9,$$
$$C_4H_9 \rightarrow C_2H_4+C_2H_5.$$

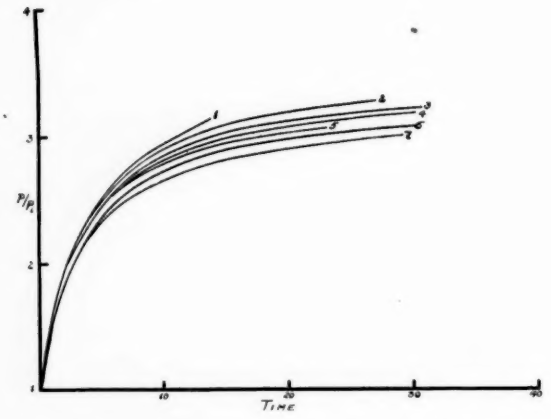

Run	Temp. °C	P_i (mm)	Time Unit (min.)
1	543	56	2.10
2	510	59	9.80
3	511	84	7.72
4	484	99	28.0
5	560	125	0.91
6	504	111	8.25
7	494	115	13.0

Fig. 1. P/P_i against time. The unit of time for each run is the time when $\Delta P = P_i/2$.

The over-all reaction would be

$$CH_3OC_4H_9 \rightarrow HCHO + C_2H_4 + C_2H_6. \quad (1)$$

Similarly the formation of butyraldehyde by a radical mechanism might be represented:

$$R + C_4H_9OCH_3 \rightarrow RH + CH_3CH_2CH_2CHOCH_3,$$
$$CH_3CH_2CH_2CHOCH_3 \rightarrow CH_3CH_2CH_2CHO + CH_3.$$

This over-all reaction would be

$$CH_3OC_4H_9 \rightarrow CH_4 + C_3H_7CHO. \quad (2)$$

Since at the beginning and well on in the reaction CH_4 is in excess of C_2H_6, it appears that C_2H_4 must also be produced from butyraldehyde. This, however, should be accompanied by more CO than appears in the analyses. For example, at 515° where $P/Pi = 1.8$, 30.1 percent C_2H_4, 16.3 of CO, 9.3 of H_2 and 16.9 of C_2H_6 are found. Assuming that H_2 and CO come principally from formaldehyde in reaction (1), then $16.3 - 9.3 = 7.0$ percent CO must have come from reaction (2). However, since in reaction (1) C_2H_4 and C_2H_6 are produced in equivalent amounts, then $30.1 - 16.9 = 13.2$ percent C_2H_4 must have been produced from reaction (2). This excess of C_2H_4 over CO suggests that butyraldehyde decomposes first into C_2H_4 and a residue containing oxygen. Specific tests for acetaldehyde gave negative results, as also did the indigo test for compounds containing the CH_3CO group. Furthermore, Rice[4] found no evidence of ketene or acetaldehyde as intermediates in butyraldehyde decomposition. It would appear likely that butyraldehyde decomposes as does acetaldehyde

$$R + C_3H_7CHO \rightarrow RH + C_3H_7CO.$$

This latter radical would be less stable than acetyl and split CO readily leaving the propyl radical which is known[5] to break down into C_2H_4 and CH_3, the latter finally yielding CH_4. The excess of C_2H_4 over CO can be partially accounted for on the basis of an observed heterogeneity of about 10 percent of the whole reaction. Davoud and Hinshelwood[6] found a heterogeneous decomposition of diethyl ether yielding ethylene and water as opposed to the homogeneous reaction yielding acetaldehyde and ethane.

A balance of reaction products suggests, therefore, that from 58 to 63 percent of the ether decomposes giving butyraldehyde, the remainder

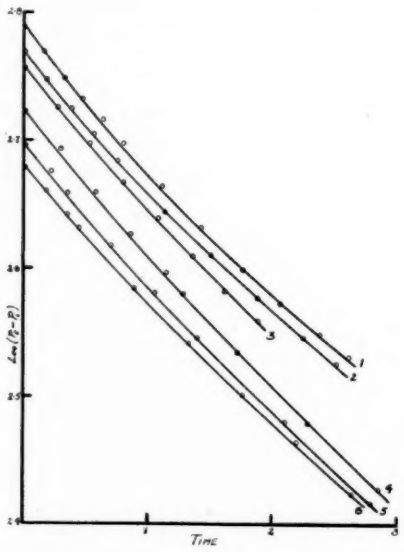

Run	Temp. °C	P_i (mm)	Time Unit (min.)
1	475	176	25.2
2	489	243	10.7
3	513	285	3.72
4	527	276	1.75
5	536	207	1.43
6	541	240	1.14

Fig. 2. Log $(P_\infty - P_i)$ against time. The unit of time for each run is the time when $\Delta P = P_i/2$.

[4] F. O. Rice, private communication.
[5] Rice, Walters, and Ruoff, J. Chem. Phys. **8**, 262 (1940).
[6] Davoud and Hinshelwood, Proc. Roy. Soc. **A171**, 39 (1939).

giving formaldehyde. The decomposition of these intermediates is fast compared with the initial ether decomposition suggesting decomposition induced by radicals from the ether.

No accurate balance of products can be made, since some material was formed just outside the furnace in the connecting tube to the reaction vessel. It is not known whether this originates from the ether or from its decomposition products. Furthermore, the analyses of the products show quite definitely that the percentages of hydrogen and ethylene decrease while that of ethane increases as the reaction proceeds; hydrogen is reacting with ethylene.

It is interesting to note that the products found and accounted for by a radical mechanism require reaction of the radical with a hydrogen atom on carbon adjacent to the oxygen, substantiating previous observations that C−H bonds in α positions (i.e., β to a C=O group) are more reactive. If hydrogen from the 1, 2, or 3 carbon atoms in the butyl group had been removed, percentages of hydrogen from 25 to 40 and unsaturates higher than ethylene would be expected.

Pressure change data

Although interpretation of the kinetics of ether decompositions from pressure-time curves is almost impossible it is nevertheless advisable, for comparison with other ethers, to note the similarities found in methyl butyl ether. A glance at Fig. 1 shows immediately that the slower reactions subsequent to the initial ether decomposition make the final pressure doubtful. To compare runs at different temperatures on the same plot, the time unit for each run is taken as the time required for the pressure to increase by fifty percent. Attempts to estimate where the reaction appeared to be going if decomposition of the intermediates did not occur led to ratios of calculated final to initial pressure varying considerably with temperature and pressure, for example, from 2.8 at 120 mm to 3.1 at 60 mm. On the other hand, ratios of actual final to initial pressure varied up to 4.0, though these values cannot be other than approximate as the pressure is still slowly rising.

A plot of log $(P_t - P_i)$ against time for different temperatures in Fig. 2 shows that the relative

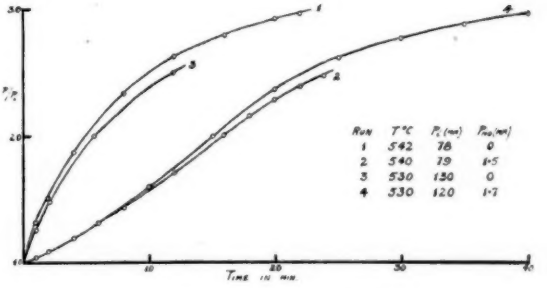

FIG. 3. Inhibition by NO.

rates of initial and secondary decompositions up to fifty percent decomposition of the ether do not change much over the temperature range studied. The rate falls off slightly faster at lower temperatures. The times for the pressure to increase 25, 50, and 100 percent of the initial pressure correspond roughly to 12.5, 25, and 50 percent of the ether decomposition. For a first-order reaction these times should be in the ratio of 0.19 : 0.45 : 1.2. The average values found for a large number of runs at pressures varying from 100 to to 200 mm and temperatures from 460° to 560°C were 0.18 : 0.40 : 1.00 indicating that the reaction is sensibly first order.[7] However, calculating the velocity constant k_i from the initial slopes of the pressure-time curves, a plot of log k_i against log P_i has an initial slope of 0.5, indicating an over-all rate of $\frac{3}{2}$ order, in the range from 25 to about 100 mm pressure. Above 200 mm the reaction is approximately first order.

The energy of activation calculated from, k_i, $t_{\frac{1}{4}}$ and $t_{\frac{1}{2}}$ at pressures from 10 to 100 mm averaged 56.6 kcal. At pressures above about 200 mm the value was 54.0 kcal. In each case a small increase in the activation energy 55.7 to 57.3 and 52.9 to 55.5 in going from k_i to $t_{i/2}$, that is as the reaction proceeds further, was observed. This may be attributed, as in similar cases,[8] to a chain inhibition by some intermediate product such as ethylene.

It should be remarked that the above data could be reproduced only by adopting a uniform procedure preliminary to a run. Prolonged pumping for several hours always produced a de-

[7] The actual data are contained in the original thesis of S. Magram in New York University Library.

[8] Fletcher and Rollefson, J. Am. Chem. Soc. **58**, 2131 (1936); F. O. Rice and O. L. Polly, J. Chem. Phys. **6**, 273 (1938).

TABLE V. *Inhibition of methyl butyl ether decomposition by NO.*

TEMP. °K	ETHER (MM)	NO (MM)	k_{inhib}	k_{inhib}/k_{norm}
758	90	0.03	0.017	0.90
773	95	13.50	0.007	0.14
773	105	6.40	0.006	0.13
773	97	3.20	0.006	0.13
773	103	1.40	0.013	0.28
773	99	0.13	0.019	0.40
776	128	6.70	0.007	0.10
786	81	0.12	0.038	0.43
787	90	11.10	0.011	0.12
790	225	3.50	0.033	0.20
793	283	2.30	0.042	0.17
793	280	4.30	0.040	0.17
793	275	0.15	0.180	0.74
798	158	2.30	0.046	0.20
803	120	1.70	0.053	0.23
803	255	8.00	0.061	0.18
807	102	2.30	0.040	0.19
808	253	0.80	0.127	0.30
809	106	3.20	0.042	0.18
809	240	0.30	0.191	0.46
809	245	8.00	0.080	0.20
812	102	0.25	0.086	0.31
813	79	1.50	0.078	0.31

composition showing a high initial rate which was not reproducible. Pumping for from five to ten minutes only, after a run, enabled subsequent ones to be repeated. To investigate further this obvious surface effect, the reaction vessel was partly filled with glass tubes with fire polished ends whereby the surface to volume ratio was increased five times. When reproducible runs were obtained with this increased surface, the rates were an average of 1.45 times faster than the normal rates. This indicates that about 10 percent of the normal reaction is heterogeneous in nature.

Inhibition by NO

The inhibited decomposition of methyl butyl ether was similar to that found by Hinshelwood and Staveley[9] in the lower ethers. Figure 3 shows two typical runs together with the uninhibited rates for comparison. The effect can be seen to be transitory from the acceleration of the rates. Whether NO is used up by the time the inflection in the curve is reached is not known. A test for cyanide made on the products collected from about eight runs was positive. This can be accounted for by decomposition of formaldoxime which is isomeric with CH_3NO. Table V contains the data for the inhibition. These data show that the effect of from 3 to 13 mm NO on the ratio of inhibited and normal rates is constant. This is probably due to a balancing of a chain inhibition and a catalytic effect by NO following a mechanism suggested by Taylor and Burton for acetaldehyde.[10] This is further borne out by the observed decreased over-all energy of activation with increased pressure as predicted by this mechanism.

A plot of log k_{inhib} against $1/T$ for a few runs with initial ether pressures from 225 to 280 mm gives an energy of activation of about 60 kcal. The mean chain length shows a small decrease with increased temperature. This would manifest itself as an increased temperature coefficient of the inhibited reaction.

Table VI presents comparative data for a number of ethers. The constancy of the energies of activation of both normal and inhibited decompositions shows that the same mechanism is probably responsible in all cases.

There is no evidence at these elevated temperatures of a hydrogen bonded ring formation. Since this might occur at room temperature, however, a preliminary photolysis[12] was attempted mainly to see if ethylene is produced in considerable amounts. The situation would be analogous to that found by Thompson and Dainton[13] in the photolysis of the alkyl nitrites. The ether vapor was exposed in a quartz reaction vessel to the radiation, mainly 2537A, from a low pressure quartz mercury arc, spiral in form and surrounding the reaction vessel. A pressure increase

TABLE VI.

ETHER	MEAN CHAIN LENGTH	E_{inhib}	E_{normal}
CH_3OCH_3	17.0 at 540°C	62.0	58.5
$CH_3OC_2H_5$	8.4 at 540°C	62.0	54.5
$CH_3OC_3H_7$	3.1 at 545°C	49.0[11]	—
$CH_3OC_4H_9$	5.0 at 536°C	60.0	54.0

[9] Hinshelwood and Staveley, Proc. Roy. Soc. **A159**, 192 (1937).

[10] Taylor and Burton, J. Chem. Phys. **7**, 414 (1939).

[11] This low value is probably due to catalysis by iodides. See Ure and Young, J. Phys. Chem. **37**, 1183 (1933).

[12] The authors wish to thank Dr. A. Gordon of this laboratory for this work.

[13] Thompson and Dainton, Trans. Faraday Soc. **33**, 1546 (1937).

indicated that decomposition occurred. The fixed gases in the products were withdrawn by means of a Toepler pump through a trap in liquid nitrogen. A relatively considerable volume was so withdrawn. Withdrawal of a second fraction was attempted at the temperature of melting *sec*-butyl chloride which should contain the ethylene. The amount of this was less than 0.1 cc. This result was checked in a second run and it was decided that the split into methyl alcohol and ethylene was not occurring and further work was abandoned.

It appears then that the principle of least motion, in predicting a direct rearrangement into product molecules of large molecules with exposed negative groups, must be restricted to such cases where, for example, an electronic resonance exists between initial and intermediate states, adding to the strength of the new bond or bonds in the intermediate.

OCTOBER, 1941 JOURNAL OF CHEMICAL PHYSICS VOLUME 9

The Pyrolysis of Formaldoxime[1]

H. Austin Taylor and H. Bender
New York University, New York, New York

(Received July 3, 1941)

Formaldoxime decomposes in a first-order reaction to give hydrogen cyanide and water at a rate $k=10^{9.5}e^{-39000/RT}$ sec^{-1}. The products react together at a slower rate to give principally carbon monoxide and ammonia although nitrogen, hydrogen, ethane and traces of unsaturate are also produced. The reaction is probably heterogeneous on a clean glass surface. It is accelerated by traces of air and by nitric oxide. These facts offer an adequate explanation of the fate of methyl radicals in nitric oxide inhibited reactions by the isomerization of the CH_3NO complex into formaldoxime.

SINCE the time of the original observation[2] that small amounts of nitric oxide were able to inhibit almost completely the decompositions of numerous organic materials, the mechanism of the action has been the subject of much experimentation but of more speculation. It is quite generally admitted that the action involves a complex formation between a radical and nitric oxide, for example, with a methyl radical, CH_3NO. It is not so generally admitted that the complex is stable. In many pyrolyses inhibited by nitric oxide, tests for cyanides in the reaction products have been obtained. In others the presence of ammonia has been demonstrated. In still other cases a white solid has been isolated and it has been suggested[3] that this solid was formaldoxime.

On the other hand however, reactions have been followed in presence of nitric oxide and no positive tests for cyanides or ammonia were found[4] wherefore decomposition of CH_3NO into methane, carbon monoxide, nitrogen and water was proposed. Further it has been suggested that the stability of the complex relative to the reactants forming it is small. Echols and Pease[5] suggested that an equilibrium is set up between the complex, nitric oxide and radicals in butane pyrolysis even at 520°C.

Although other interpretations may be offered for some of the observations that have led to the above suggestions, the variety of these suggestions indicates a lack of knowledge of the stability of possible isomers of the complex. For the complex CH_3NO, the most obvious isomers are formamide and formaldoxime. Of the latter little is known at all of its decomposition products and according to Sherman[6] formamide

[1] Abstract from a thesis submitted in partial fulfillment of the requirements for the degree of Doctor of Philosophy, New York University, June, 1941.
[2] Staveley and Hinshelwood, Proc. Roy. Soc. **A154**, 335 (1936).
[3] Linnett and Thompson, Trans. Faraday Soc. **33**, 874 (1937); Davis, Jahn, and Burton, J. Am. Chem. Soc. **60**, 10 (1938); Taylor and Jahn, J. Chem. Phys. **7**, 470 (1939).
[4] Staveley, Proc. Roy. Soc. **A162**, 557 (1937).
[5] Echols and Pease, J. Am. Chem. Soc. **59**, 766 (1937).
[6] Sherman, Am. Chem. J. **20**, 226 (1904).

TABLE I.

TIME MIN.	$T=412°$ $P_i=103.5$ MM ΔP (MM)	$T=385°$ $P_i=68.5$ MM ΔP (MM)	$T=376°$ $P_i=81.0$ MM ΔP (MM)	$T=350°$ $P_i=129.3$ MM ΔP (MM)
1.0	6.4	0.2	0.5	0.3
1.5	10.5	0.6	0.9	—
2.0	13.8	1.4	1.5	0.8
2.5	16.7	1.6	1.9	—
3.0	19.5	2.2	2.4	1.0
3.5	22.0	2.9	2.9	—
4.0	24.9	3.6	3.8	1.9
4.5	26.8	4.0	—	—
5.0	29.0	—	4.7	2.8
5.5	31.0	5.4	—	—
6.0	33.0	5.9	5.5	3.8
7.0	34.5	6.9	6.5	4.8
8.0	35.3	7.7	—	—
9.0	39.2		—	6.5
10.0	41.9		8.9	—
15.0	51.2		10.8	9.8

gives ammonia and carbon monoxide on distillation and when heated above 195°C yields also hydrogen cyanide and water. Whether isomerization from one to the other is possible is not known.

The first attempt to follow the mechanism of nitric oxide inhibition directly was made by Thompson and Meissner.[7] They followed the change in the absorption spectrum during reaction of a mixture of nitric oxide and dimethyl ether. It was found that the nitric oxide bands progressively weakened as ether decompositions progressed and that ammonia bands appeared. The disappearance of the nitric oxide bands paralleled the resumption of normal ether decomposition. It was suggested that formaldoxime might be the intermediate. Using diethyl ether in a similar experiment new bands appear which could be attributed to methylamine and the following reaction was proposed:

$$C_2H_5+NO\rightarrow CH_3NH_2+CO.$$

Alternatively an unstable nitroso compound may have been present since, when the reaction products were frozen out a blue solution resulted. The production of carbon monoxide might however result from formamide, the corresponding ammonia reacting with radicals to give methylamine. The evidence therefore is not unequivocal and it was hoped that a study of the decomposition of formaldoxime might throw light on the whole subject.

[7] Thompson and Meissner, Nature **139**, 1018 (1937).

EXPERIMENTAL

Formaldoxime was prepared by the method of Scholl.[8] Hydroxylamine hydrochloride was dissolved in a minimum amount of water, completely neutralized with sodium carbonate and cooled below 5°C in an ice bath. Formaldehyde solution is added with constant stirring, the low temperature being maintained. A heavy white precipitate soon separates. The mixture is allowed to stand in an ice box for a few hours to ensure complete reaction and filtered on a Buchner funnel. The solid is washed with water at about 50°C until free of chlorides and dried in air. The product may be purified by sublimation below 100°C without decomposition. The white solid is a polymer of formaldoxime.

To determine the molecular state of the vapor from this solid, the molecular weight was determined by observing the pressure at which a known weight of the polymer as vapor occupied a predetermined volume at the chosen temperature. The results of three such determinations at about 100°C were 46.9, 45.4 and 46.0. The molecular weight of CH_2 : NOH is 45.0, hence it may be concluded that the vapor is completely depolymerized at 100°C.

In preliminary bomb tube experiments the presence of hydrogen cyanide, ammonia, and carbon monoxide was established among the products of decomposition. The bomb tubes after heating at about 400°C for varying lengths of time showed on cooling heavy brownish deposits which were attributed to polymerization of hydrogen cyanide and drops of liquid which persisted on standing. The monomeric formaldoxime is a liquid under ordinary conditions but polymerizes on standing. The liquid therefore was

TABLE II.

TEMP. °C	$k\times10^4$ SEC.$^{-1}$	TEMP. °C	$k\times10^4$ SEC.$^{-1}$
413	10.8	385	3.0
412	11.5	381	2.4
412	10.1	378	2.4
412	10.2	378	2.3
408	10.0	376	2.2
408	8.8	375	2.1
405	7.5	374	1.9
401	6.6	370	1.4
398	5.1	365	1.2
386	2.9	350	1.2

[8] Scholl, Ber. **24**, 573 (1891).

taken to be water. A small amount of unabsorbable gas was always observed. It was decided to study the pyrolysis using a static method by following the pressure change during decomposition making subsequent analyses of the products.

A 500-cc Pyrex reaction vessel in an electrically heated furnace was connected to a constant volume manometer, and through a mercury cut-off to the formaldoxime reservoirs, diffusion pump system and to a Toepler pump. To prevent condensation, all the connecting tubing was heated to about 100°C. As a lubricant on the heated stopcocks a plasticizer, di-*o*-xenylmonophenylphosphate was used, the reaction system during a run being closed by mercury. The solid polymer of formaldoxime was vaporized into a liter storage bulb kept in boiling water. The reactant was drawn from this bulb as required.

In the early experiments before the mercury cut-off was introduced and before the plasticizer was used as lubricant very erratic results were obtained. These were traced in part to leaks due to the heated stopcocks. The accelerating effect of traces of air may be significant if acting as chain starters. On the other hand a clean glass surface had an accelerating effect. The rate of reaction decreased steadily to a reproducible limit as successive reactions are carried out. Alternatively this condition could be obtained by decomposing acetone for a prolonged period in the reaction vessel prior to a run. The admission of air to such a prepared surface completely spoiled the reproducibility, subsequent rates being again high. The reaction is undoubtedly in part heterogeneous on a clean glass surface though whether the poisoning of the surface by this method was complete was not tested by poisoning in like manner a more extended surface.

At the conclusion of a run the mercury in the cut-off was lowered and the products withdrawn by means of the Toepler pump for analysis.

Results

Experiments were made over the temperature range from 350° to 415°C. The ratio of final to initial pressure varied from 1.8 to 1.9. Analysis indicates that the principal primary products are hydrogen cyanide and water and that a 2 to 1 ratio for final to initial pressure should result. The most likely explanation of the lower final ratio is that hydrogen cyanide is a reactive substance and especially in presence of water is known to polymerize. Analytical data presented later show that complicating secondary reactions of hydrogen cyanide and water become significant later in the over-all reaction.

Table III.

Temp. °C	Time	V_c/V_m
415	Zero	10.0
415	2 days	3.1
415	3 days	2.2
435	20 min.	8.0
450	10 min.	7.7
450	12 hr.	2.2
450	3 days	1.3

At the lowest temperatures studied the reaction shows a short induction period, the cause of which could not be found. At 370°C and above, however, the induction period is too short to be noticed and plots of the logarithm of the formaldoxime pressure against time are initially linear. The reaction interval during which linearity of this plot persists increases with temperature. At 370°C the reaction deviates from first order after about one-fifth of the time for total decomposition, while above 400°C the reaction is first order to almost the half-life. A possible explanation of the falling off in the rate and its variation with temperature again lies in the polymerization of hydrogen cyanide formed. At higher temperatures a relatively higher concentration of monomer will be present and the normal pressure increase will persist to a greater extent of decomposition of the formaldoxime. Alternatively at lower temperatures the higher proportion of polymer causes a less rapid total pressure increase and the reaction appears to fall off. In Table I are given some illustrative data of the observed pressure increase.

Assuming the reaction to be the simple two-mole product for one of reactant, the pressure of undecomposed formaldoxime at any time may be taken as the initial pressure less the observed pressure increase. Velocity constants were calculated from the slope of the best straight line through data of the logarithms of the pressure

against time. A summary of these constants is given in Table II.

These data give a good straight line when plotted as log k against $1/T$ and the slope of the line corresponds to an energy of activation of 39 kcals.

The preliminary analytical work having shown the presence of hydrogen cyanide, ammonia and water among the products of decomposition it was realized that these would condense or be dissolved in passage through the Toepler pump system and would not be collectible entirely for analysis. To estimate the approximate amount of such absorbable gases the products withdrawn by the Toepler were washed with dilute acid and alkali and their volume V_m measured. Knowing the volume of the reaction system the volume V_c of gas, theoretically to be withdrawn, can be calculated from the pressure and temperature in the reaction vessel. Table III gives several values of the ratio of V_c/V_m at various temperatures for the gases withdrawn at the times indicated. These times are measured from the time that reaction appears to be complete as judged by the pressure change.

The ratio V_c/V_m is seen to decrease with time, that is, the proportion of gas not removed by acid and alkaline washing increases with time. If the only products of formaldoxime decomposition were hydrogen cyanide and water, V_c/V_m would be infinite. If however these can react further to give carbon monoxide and ammonia, V_c/V_m for complete reaction would be unity. The observed trend of the ratio indicates that hydrogen cyanide and water may react further. This is borne out by some rough analyses of the washed gases which show that when the ratio V_c/V_m is high the percentage of carbon monoxide is only about 40. As V_c/V_m decreases the percentage rises to over 60. The reaction is by no means simple since about 20 percent of the gas is nitrogen and small amounts are present of hydrogen, unsaturates and a hydrocarbon, the average ratio of contraction to carbon dioxide produced on combustion of which indicated it to be ethane. That the increase in production of carbon monoxide is probably not due to a direct decomposition of formaldoxime into carbon monoxide and ammonia simultaneously with decomposition into hydrogen cyanide and water is inferred from separate experiments. Equimolecular mixtures of hydrogen cyanide and water were sealed in bomb tubes and heated for varying periods of time in a furnace at 450°C. The tubes were opened under water. The water on analysis showed the presence of ammonia as well as cyanide. The water only partly filled the tubes showing that insoluble gases had been produced. These on analysis showed an average of 61 percent carbon monoxide, 20 percent nitrogen, 15 percent hydrogen, 4 percent ethane and traces of unsaturate. These values are in close agreement with those found when the products from formaldoxime are allowed to remain in the furnace for some time after pressure change had ceased. Finally to confirm that the nitrogen and other products are produced from hydrogen cyanide and water and not from carbon monoxide and ammonia, bomb tubes of the latter mixture were heated as previously for several days. On cooling a slight white deposit formed on the sides of the tube. On opening under water the deposit dissolved. The solution showed the presence of ammonia but no cyanide. The insoluble gas was almost pure carbon monoxide.

Discussion

The pyrolysis of formaldoxime is seen to involve a primary dissociation into hydrogen cyanide and water with an accompanying pressure change. These products react further, but more slowly, to produce chiefly carbon monoxide and ammonia by a reaction almost devoid of pressure change. The velocity constants previously calculated thus represent the rates of the primary dissociation and the activation energy calculated from them is for the reaction:

$$CH_2NOH \rightarrow HCN + H_2O.$$

The rate of this reaction may thus be expressed:

$$k = 10^{9.5} e^{-39000/RT} \text{ sec.}^{-1}.$$

The low value of the frequency factor, indicating that the process of activation is accompanied by an appreciable decrease in entropy, is not unexpected in view of the restriction of motion that must exist in the activated formaldoxime when about to dissociate into hydrogen cyanide and water, over that in the normal molecule.

The value of the activation energy 39 kcal. is close to that found by Steacie[9] for the N−O bond in alkyl nitrites namely 37.7 kcal. This too indicates that it is the N−O bond in the activated complex which breaks.

The subsequent reactions of hydrogen cyanide and water must remain for the present matters for conjecture. It is known[10] that hydrogen cyanide forms several polymers. One of these, diiminoethylene, HN=C=C=NH might readily react with water to produce carbon monoxide and ammonia. Another, diamino maleic dinitrile

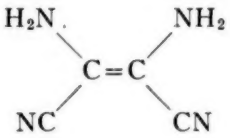

might conceivably be a source of hydrocarbons, while the complete pyrolysis of higher polymers has been reported[11] to yield nitrogen and hydrogen.

The presence of ethane in the final products suggests a decomposition of formaldoxime into nitric oxide and a methyl radical. Many tests were made for nitric oxide and all proved negative. Furthermore when nitric oxid was purposely added in very small quantities to formaldoxime, a marked increase in the rate of pressure change was observed. This increase was so marked that in one attempt to introduce nitric oxide when formaldoxime was already partially decomposed, a violent explosion ensued, shattering the apparatus. The work was not pursued and no attempt was made to compare the products from formaldoxime in presence and absence of nitric oxide. The reaction, however, appears to be similar to that in presence of small amounts of air where also a marked acceleration of the rate of pressure increase is observed. If nitric oxide were produced during the course of the reaction an auto-acceleration would be expected. The induction period at lower temperatures is the only observation of any such effect. Even if this was the correct explanation of the presence of ethane and of the induction period, the amount of formaldoxime decomposing in this manner must be small and the effect of the nitric oxide must be that of a chain inducer. The whole possibility seems doubtful in view of the formation of ethane from hydrogen cyanide and water.

The problem of the fate of methyl radicals in presence of nitric oxide can thus adequately be explained on the basis of the formation and subsequent decomposition of formaldoxime. The alternative production of formamide is not so satisfactory in accounting for many of the observations in nitric oxide inhibited reactions. Thus formamide is liquid whereas a white solid is usually observed. It decomposes readily to give ammonia and carbon monoxide at lower temperatures without any trace of hydrogen cyanide while at higher temperatures only small traces of cyanide can be found. Positive tests for cyanide are much more frequent than for ammonia in nitric oxide inhibitions.

[9] Steacie and Shaw, J. Chem. Phys. **3**, 344 (1935).
[10] Bedel, Bull. Soc. Chim. **35**, 339 (1924).
[11] St. Claire Deville, J. über die Forts. Chem. 307 (1863).

Double Refraction of Flow Studies with Methyl Methacrylate Polymers in Solution[1]

A. J. DE ROSSET[2]
University of Wisconsin, Madison, Wisconsin
(Received April 23, 1941)

An apparatus for the measurement of double refraction of flow is described. The magnitude of birefringence, expressed as the rotation of the plane of polarized light, may be measured to 0.05° under the best conditions with the assembly. The vortical angle and double refraction of flow of dioxane solutions of a series of fractionated polymers of α-methyl methacrylate have been measured at 25° over a concentration range of from one gram per liter to 50 grams per liter, depending upon the polymer under investigation. The specific birefringence, referred to the viscosity of the solvent, is a constant characteristic of each polymer in sufficiently dilute dioxane solutions. With the possible exception of behavior in such dilute solutions, the vortical angle is dependent upon concentration. Values of the rotary diffusion constant are calculated for each polymer from measurements of the vortical angle taken in dilute solutions. The lengths of the polymers are calculated from the rotary diffusion constants. They vary from 890A to 1880A. The shape and structure of the polymers are discussed from the point of view of their electrostatic and steric properties as evidenced by a molecular model. Tentative values of molecular weight and of length to width ratio are assigned. The viscosity of dilute dioxane solutions of the polymers has been measured at 25°. The specific viscosity increment at infinite dilution is estimated by extrapolation. This quantity is a linear function of the square of the length to width ratio, in partial confirmation of several theories of the viscosity of macromolecular solutions.

1. INTRODUCTION

AMONG the many high molecular weight substances which have been investigated recently with the new techniques of colloid chemistry, a large number are found which possess elongated structural units. In dilute solutions the behavior of these macromolecules is described by the molecular kinetic theory. There are several procedures which may be followed in studying these dilute solutions to give information about the length and length to width ratio of the solute molecules. Three of them, sedimentation analyses,[3] dispersion of dielectric constant,[4] and viscosity,[5] have been the subject of much theoretical and experimental development. Less well-grounded from a theoretical viewpoint, and at the present time more difficult for experimentation, is the measurement of the double refraction exhibited by such solutions when they are subjected to a mechanical shearing stress. In this research the attempt was made to observe the flow double refraction in dilute dioxane solutions of methyl methacrylate polymers and to estimate the size and shape of such polymers from these data.

2. THEORY

Double refraction studies are usually made in the Kundt cell. It consists of two concentric cylinders, one of which may be rotated at a uniform speed. The solution under investigation is placed in the annular space between the cylinders. A beam of plane polarized light is passed through this cylindrical shell of liquid in the direction parallel to the axis of rotation. When the solution is sheared, it exhibits birefringence, which may be measured according to the classical method as the apparent rotation of the plane of the polarized light, by using a quarter-wave plate compensator.

In determining the birefringence of non-dichroic solutions, both the amount and direction of double refraction must be considered. If the plane of the incident polarized light is rotated through 360°, the magnitude of birefringence will pass through four maxima at intervals of 90°. One pair of maxima will make an angle equal to or less than 45° with the direction of flow. This

[1] More complete details of this work are to be found in the thesis of Armand J. de Rosset submitted to the faculty of the University of Wisconsin in partial fulfillment of the requirements for the Ph.D. degree in June, 1939.
[2] Present Address: Universal Oil Products Company, Riverside, Illinois.
[3] Svedberg and Pedersen, *The Ultracentrifuge* (Clarendon Press, Oxford, 1940).
[4] P. Debye, *Polar Molecules* (Chemical Catalog Company, New York, 1929); Perrin, J. de phys. et rad. **5**, 497 (1934).
[5] Staudinger, *Die hochmolekularen organischen Naturstoffe* (Berlin, 1932); Mark, *Physical Chemistry of High Polymeric Systems* (Interscience Publishers, New York, 1940).

angle is known as the vortical angle and will be designated by the symbol ψ. The magnitude of the maxima is the amount of double refraction of the solution, and will be designated by the symbol B. From the theory of birefringence it follows that

$$B = Z\lambda/180h. \quad (1)$$

In this equation Z is the observed rotation of the plane of the polarized light in degrees, and λ and h are the wave-length of light used and the depth of medium traversed, respectively, measured in the same units.

In this report use is made of a quantity S, defined as $S = B/G\eta_0$. In this expression G is the velocity gradient between the cylinders, and η_0 is the viscosity of the solvent. If the solvent alone shows a slight birefringence B_0 a similar expression holds,

$$S_0 = B_0/G\eta_0.$$

Then the specific birefringence of the solute is defined as

$$D = (S - S_0)/c, \quad (2)$$

where c is the weight concentration of solute in grams per liter.

Practically all modern theories of double refraction of flow of solutions presuppose that the elongated solute molecules are oriented by the velocity gradient through the solution. The resulting birefringence may be attributed to the intrinsic optical anisotropy of the solute particles; or it may arise from their shape alone, as was pointed out by Wiener.[6] The former type of double refraction is "intrinsic," the latter is "form" double refraction. The amount of form double refraction depends on the refractive index of the solvent and, from Wiener's theory, should vanish when this is equal to the refractive index of the solute particles. Sadron,[7] however, deduces a somewhat different situation.

The first step in developing an orientation theory of double refraction is to determine the angular distribution of the particle axes under the opposing influences of the velocity gradient tending to orient the particles, and of Brownian motion tending to disarray them. This has been done by Boeder,[8] who solves graphically the two-dimensional equation of forced diffusion,

$$\theta\partial^2\rho/\partial\phi^2 + G\partial(\rho \sin^2\phi)/\partial\phi = 0. \quad (3)$$

Here, θ is the rotary diffusion constant, ρ is the direction density of particle axes, and ϕ is the angle between a particle axis and direction of flow. This equation assumes that the particles are rigid, homogeneous, and that they are long enough to approximate liquid lines. It also presupposes that the particles do not interact to prevent independent rotary diffusion and that there is no other orienting influence but that of the velocity gradient. Boeder's solution is given in Table I, where B and ψ are given as functions of the ratio G/θ. The quantity B has been normalized to 2π as the maximum possible amount of birefringence. From the data in the third column, it is possible to determine immediately the rotary diffusion constant of any system of macromolecules which satisfies Eq. (3) from an observation of the vortical angle at any given gradient.

Kuhn,[9] using much the same hydrodynamic treatment which he employs in his theory of viscosity, relates the rotary diffusion constant to the length of the particle by the equation

$$\theta_0 = \theta\eta_0 = 8kT/\pi s^3, \quad (4)$$

in which θ_0 is the rotary diffusion constant reduced to unit viscosity of solvent η_0, k is the Boltzmann constant, T is the absolute temperature, and s is the length of the particle, assumed to be much larger than the width. Kuhn also relates the specific birefringence of the solute to the rotary diffusion constant by an equation which may be reduced to the simple form

$$D\theta_0 = \text{constant}. \quad (5)$$

The constant is valid for a homologous series of macromolecules. One assumes that the total anisotropy of the macromolecules is proportional

TABLE I. *Boeder's solution of the distribution problem.*

G/θ	B	ψ	G/θ	B	ψ
0.0	0.0	45.00°	3.5	2.000	25.83°
0.5	0.390	41.45°	5.0	2.400	22.00°
1.0	0.755	38.25°	7.5	2.770	17.50°
2.0	1.367	32.22°	10.0	3.020	15.00°

[6] Wiener, Physik. Zeits. **5**, 332 (1904).
[7] Sadron, J. de phys. et rad. **8**, 481 (1937).
[8] Boeder, Zeits. f. Physik **75**, 258 (1932).
[9] Kuhn, Zeits. f. physik. Chemie **A161**, 1 (1932).

to their mass. This is equivalent to assuming that the maximum potential birefringence of the solution (complete orientation of macromolecules) is proportional to the weight concentration.

Sadron[7] has recently considered the effect of solvent, neglected by Boeder and by Kuhn. His general equation for double refraction flow is

$$\frac{1}{N}\frac{B\theta_0}{G\eta_0}\frac{n_0}{n_0^2+2} = \frac{\pi}{3}\frac{a^2-b^2}{a^2+b^2}[(\sigma_1-\sigma_2)+\Delta'(e_a\sigma_1-e_b\sigma_2)], \quad (6)$$

where N = number of molecules per unit volume; a, b = major and minor axes of molecule, considered as an ellipsoid of revolution; σ_1, σ_2 = optical polarizabilities of the molecule along these axes; e_a, e_b = geometrical constants of the ellipsoid; n_0 = refractive index of the solvent; $\Delta' = (n_0^2-1)/(n_0^2+2)$. The term involving $(\sigma_1-\sigma_2)$ represents intrinsic double refraction, while that involving $(e_a\sigma_1-e_b\sigma_2)$ represents form double refraction. The denominator of the left-hand side should be multiplied by a factor of 3 to correct for an algebraic error copied from an earlier paper by Langevin. We find, in attempting to reproduce Sadron's integrations, that apparently an additional factor of 4 should be introduced into the denominator as well.

Equation (6) predicts that a solution of optically isotropic macromolecules will always show double refraction of flow, whatever the solvent. That is, there will exist no solvent of critical refractive index in which the birefringence will vanish. This conclusion is inconsistent with that of Wiener who states that form double refraction (which is all that need be considered when dealing with intrinsically isotropic particles) will vanish when the solute and solvent have the same refractive index. Wiener's theory is valid, however, only for particles much smaller than the wave-length of light. Many macromolecules do not satisfy this condition.

Equation (6) may be reduced to a form comparable with Eq. (5) by assuming as before that the anisotropy of the macromolecule is proportional to its mass. One obtains for a long anisotropic particle

$$D \propto (1/\theta_0)[1-\Delta'/\Delta'_c], \quad (7)$$

where Δ'_c refers to the refractive index function for the critical solvent in which double refraction of flow disappears.

3. Apparatus and Methods

For the viscosity measurements described in this report the Washburn-Williams modification of the Ostwald viscometer is used. The efflux time for water is 190 seconds at 25.00°C using a 25 cc volume of liquid. The equation for kinematic viscosity in stokes k_v is

$$k_v = 4.87\times10^{-5}t - 0.056/t,$$

where t is the time of efflux in seconds. Density measurements, required for the calculation of absolute viscosities, are made in a single bulb Ostwald pycnometer of volume nearly 8 cc.

The apparatus used for measuring the double refraction of flow of polymeric methyl methacrylate solutions consists essentially of a Kundt cell and a precision polarimeter mounted horizontally on an optical bench.

The outer cylinder or stator of the Kundt cell is brass with an inner radius of 5.293 cm and a length of 10.71 cm. It has a permanently attached base plate and a cover plate which may be removed to permit insertion of the inner cylinder, or rotor. The base plate of the stator is provided with a recess which holds a bronze bearing and the rear end of the rotor shaft. The cover plate may be firmly clamped to the stator by a large threaded bronze ring. It is drilled through the center and equipped with a collar through which passes the front end of the rotor shaft. This collar houses the packing and packing nut, a Torrington No. T-201 ball race, and a large set screw which holds the ball race firmly against a shoulder on the rotor shaft. The packing used in the experiments on dioxane solutions was woven cotton wick material which had been soaked in a mixture of glycerol and 300-mesh graphite. The cover plate is also equipped with an inlet tube and filling bulb, and a gauge to observe the level of the solution in the cell.

Recessed slits, 3 mm long, are cut through both cover and base plates near their periphery to correspond to the gap between the cylinders. Brass window holders are held in the recesses by three screws. Windows cut from strain-free

optical glass are cemented into the holders with glycerol-litharge cement. When the window holders are assembled to the cell, the screws are tightened evenly to preclude any strains which would make the windows double refracting. The windows are aligned by a brass pin in the cover plate which drops into a hole to correspond in the rim of the stator.

The stator is wrapped with $\frac{3}{8}''$ copper tubing through which water at $25° \pm 0.03°$ from a large reservoir is driven by a circulatory pump.

The rotor is constructed of phosphor bronze tubing, the brass end plates and steel shaft being soldered on. It has an outside diameter of 5.266 cm and a length of 10.69 cm. The gap between the cylinders is 0.0268 cm, which is small enough to permit high velocity gradients to be attained before turbulent flow sets in. Clearance of the rotor at the base and cover plates of the stator may be adjusted by a set screw in the base plate which regulates the height of the bronze bearing.

The rotor is driven at uniform speed by a one-half horse power induction motor. The speed may be varied continuously from 360 r.p.m. to 3600 r.p.m. by a DT-$\frac{1}{4}$ Transitorq unit which is attached directly to the drive shaft of the motor. Lower speeds are made available by a 3–1 reduction pulley. The power is transmitted from the Transitorq unit to the rotor by a flexible shaft whose length is 6′ and core diameter is $\frac{3}{8}''$. A stroboscope is mounted at the Transitorq end of the flexible shaft. Its accuracy in determining speeds of rotation, as checked against a tachometer, is 0.5 percent.

The optical system consists of light source, filter, slit, collimating lens, polarizing Nicol, Kundt cell, mica quarter-wave plate compensator, mica half-wave plate Chauvin half-shadow, analyzing Nicol, and telescope.

The light source is Type H-3 85-watt General Electric Company mercury vapor lamp. The mercury green line (5461A) is isolated by Corning glass filters Nos. 351, 430, and 512. The filters are mounted on the stand supporting the slit which is usually set at 0.04–0.06 cm. The lens is placed at its focal length, 15 cm, from the slit to obtain a parallel beam.

The polarizing and analyzing Nicols of the polarimeter may be locked together in the crossed position and rotated as a unit for the purpose of determining the vortical angle. The coupling is made by two identical brass drums which operate on a drill rod steel shaft. These drums are connected by piano wire to two larger identical drums which rotate with the Nicol prisms. Turning the steel shaft causes the two Nicols to rotate without changing appreciably their orientation over a rotation of 90°.

Since the vortical angle is referred to the direction of flow, and the latter is horizontal when the Kundt cell is operated with its windows at the top, the horizontal position of either polarizer or analyzer must be found. This calibration was made by suspending a glass plate vertically in front of the analyzer. Then the planes of the glass and light source were adjusted to reflect vertically plane polarized light into the analyzer, which was rotated to extinction. This experiment determined the reading on the polarimeter scale at which the principal plane of the analyzing Nicol is horizontal.

The assembled cell is filled with solution through the filling tube, by a capillary attached to a 40-cc separatory funnel which serves as reservoir for the solution during an experiment. Bubbles are flushed out through two small holes drilled through the window holders. These holes are closed with wooden plugs when the cell is in operation. When filled, the cell is clamped horizontally on the optical bench and connections are made to the water lines and flexible shaft. The Transitorq is set at any desired speed. The vortical angle ψ is determined by removing the compensator and rotating the locked crossed Nicols from the reference horizontal position to the nearest minimum. To measure the amount of birefringence, the rotor is stopped, and the crossed Nicols are rotated 45° from the minimum just found. The compensator is inserted and rotated to extinction. The polarizer is locked in position and the analyzer uncoupled. The rotor is again started and the analyzer alone is rotated to extinction. Thus, rotation of the plane of the polarized light in degrees is measured on the polarimeter scale. It is the angle Z of Eq. (1).

The accuracy of the determination of the vortical angle depends upon the amount of birefringence involved, since this determines the contrast between maxima and minima observed

as the crossed Nicols are rotated. When the angle Z is less than 0.5°, the maxima and minima are too broad to distinguish. For values of Z in the vicinity of 1.0°, ψ may be determined with a probable error of 5° or less. The angle Z itself may be determined with an accuracy of $\pm 0.05°$ under the best conditions. Eye fatigue, or any factors which cut down the light intensity, will reduce this accuracy.

4. Preparation of Materials

A series of polymers of α-methyl methacrylate was prepared by heating the monomer in solution according to a method suggested by Strain.[10] The reaction was carried out under a number of different conditions to obtain products of various degrees of polymerization. The relative degree of polymerization was roughly estimated by measuring the viscosity of 0.1 percent solutions of the products in dried dioxane. Of nine polymers prepared, five were used for the double refraction experiments. These will be designated in order of increasing molecular weight as A, B, C, D, and E.

Since it is essential that the samples be as homogeneous as possible, various techniques were employed to reduce the polydispersity. The degree of polymerization was found to increase during the course of a reaction. Hence, one useful technique involved the removal of the product at various stages of the reaction. This was possible in the case of the last four polymers because the solvent used, aqueous methanol, precipitates the polymer as it is formed.

Polymer A

Ten cc of monomer and 40 cc of commercial dioxane were heated at 65°±1°C under reflux. Ten cc of monomer was added at a rate of 1 cc per five hours. This rate corresponded to the initial rate of the reaction as determined by preliminary experiments. By keeping the monomer concentration constant in this way it was hoped to decrease the polydispersity of the product. When all the monomer had been added, the solution was diluted with a large excess of acetone, and the polymer was precipitated with water. It was then washed with water and dried at 85°C.

[10] Strain, Ind. Eng. Chem. **30**, 345 (1938).

Polymers B and C

Fifty cc of monomer and 200 cc of 50 percent by volume aqueous methanol, together with 1 percent of benzoyl peroxide figured on the basis of the monomer were heated under reflux at 65°C. After an induction period of about two hours, precipitation commenced. At the end of three hours the precipitate was removed, washed with methanol and water, and dried. This fraction represented a portion of the total yield included between 0 percent and 40 percent. It is designated as polymer B.

The reaction was repeated, the cloudy supernatant liquid being decanted into a clean reaction flask at the end of $2\frac{1}{2}$ hours. At the end of an additional $1\frac{1}{2}$-hour period, more precipitate had formed in the fresh flask. This material, designated as polymer C, was washed with methanol, water, and dried. It represented a fraction of the total yield included between 50 percent and 80 percent.

Polymers D and E

The conditions for the preparation of these polymers were the same as for polymers B and C, except that the catalyst, benzoyl peroxide, was omitted. Precipitation began at the end of 50 hours, and by 64 hours the reaction had gone to completion. The total product was separated into two parts, a hard central lump, and a soft material which had accumulated on the walls of the flask. The latter fraction, designated as polymer D, was washed with water and dried. The aggregated material was further fractionated by dissolving it in acetone and diluting the solution with two volumes of hot ethanol. As the solution cooled to room temperature, the polymer precipitated. After four hours the precipitate which had settled was removed, washed, and dried. This fraction is designated as polymer E.

The dioxane which was used as solvent in the double refraction measurements was carefully purified according to a procedure suggested by Weissberger and Proskauer.[11] The material generally showed upon distillation a boiling range of less than 0.3°. Ten samples gave $d_4^{25}=1.0273$, and $\eta_{25}=0.01186$ as average values.

[11] Weissberger and Proskauer, *Organic Solvents* (Clarendon Press, Oxford, 1935).

The viscosities of 0.1 percent solutions of polymers A, B, C, D and E in dioxane at 25°C were 0.0125, 0.0140, 0.0147, 0.0162 and 0.0191, in order. They are here expressed in absolute units.

5. Experimental Results

Observations of vortical angle and birefringence were made at 25° for dioxane solutions of the five methyl methacrylate polymers over a range of concentration from 1 gram per liter to 50 grams per liter, and over a range of velocity gradient from 4000 sec.$^{-1}$ to 15,000 sec.$^{-1}$.

In all cases the magnitude of the birefringence was found to be proportional to the velocity gradient. This law has been shown to hold for a large number of systems (polystyrene, nitrocellulose,[12] ω-hydroxy decanoic acid polyesters,[13] tobacco mosaic virus protein,[14] and a large number of pure liquids.[15] Such behavior is predicted by Boeder in his solution of Eq. (3), provided the ratio G/θ is small.

From this fact it follows that the birefringence S previously defined is a constant for any given solution. In Fig. 1, S is plotted for each of the five polymers as a function of concentration. The graph shows that in dilute solutions S varies linearly with concentration, and that all the lines extrapolate to the point marked S_0 at infinite dilution. This point should represent the magnitude of the solvent birefringence. Actually, S_0 for dioxane was found to be 0.13×10^{-10} by averaging the results of 57 measurements taken at a velocity gradient of 6200 sec.$^{-1}$. This value agrees within experimental error with that obtained by extrapolating S to zero concentration. It is concluded, therefore, that the specific birefringence D is a constant characteristic of each polymer in a given solvent.

Largely as a matter of convenience in the evaluation of the data, the plots of Fig. 1 have been drawn as broken lines. The slopes of the S *vs.* c curves are constant in regions of low concentration and give the specific birefringence D for the several polymers, after correction has been made for the solvent birefringence (Eq. (2)).

[12] Signer and Gross, Zeits. f. physik. Chemie **A165**, 161 (1933).
[13] Quimby, dissertation, University of Wisconsin (1937).
[14] Mehl, Cold Spring Harbor Symposium on Quantitative Biology, Vol. 6 (1938), p. 218.
[15] Sadron, J. de phys. et rad. **7**, 263 (1936).

The specific birefringence ceases to be constant in the more concentrated solutions and it increases with concentration. (Additional data for polymers A and E are not shown in the figure for lack of space, but are indicated by the direction of the arrows.)

Preliminary to any measurement of B, the vortical angle ψ must be determined. Table II gives the average values of the vortical angles for solutions of the five polymers, measured over a range of velocity gradients. The data in italics are the G/θ ratios corresponding to each vortical angle, as interpolated from Table I.

One would expect, from Boeder's theory, that the vortical angle should be independent of concentration. Actually it shows a marked concentration dependence, a phenomenon which was also observed by von Muralt and Edsall[16] in working with muscle globulin. However, it has just been demonstrated that the specific birefringence varies in solutions of appreciable concentration. Therefore, by Eqs. (5) or (7), θ should vary and hence also ψ. With this consideration in mind we have selected for the average only those values of ψ which have been measured in the concentration region where D is constant. Unfortunately, in this concentration region where one would expect ψ to remain constant, experimental observations are less accurate, and its exact behavior cannot be determined with the present apparatus. One factor which might well cause variation in the vortical angle even below the critical concentration is the additive effect of the vortical angle of a slightly birefringent solvent, which is always 45°. Sadron[17] has shown that for such a two-component system

$$\tan 2\psi_{obs} - \tan 2\psi_1 = (B_0/B_1)\sec 2\psi_1 \qquad (8)$$

where the subscript 1 refers to the solute and subscript 0 to the solvent. If B_0 is less than $\frac{1}{10}$ the observed birefringence, then the effect of the solvent on the vortical angle is within the experimental error.

The rotary diffusion constants of the five polymers in radians per second were calculated by dividing the G/θ ratios (Table II) into the corresponding values of the velocity gradient

[16] von Muralt and Edsall, J. Biol. Chem. **89**, 315, 351 (1930).
[17] Sadron, J. de phys. et rad. **9**, 381, 384 (1938).

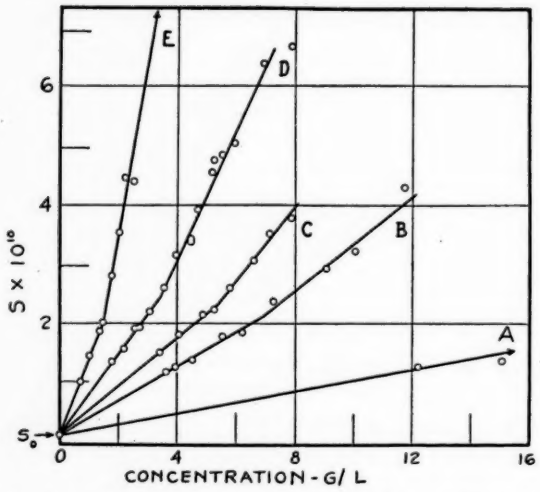

FIG. 1. Birefringence of methyl methacrylate polymers in dioxane solution, per unit velocity gradient, per unit viscosity of solvent as a function of concentration.

and averaging the results. In Table III they have been reduced to unit viscosity by multiplying by 0.0119, the absolute viscosity of the solvent.

In the course of assembling the birefringence data, the viscosity of each solution was measured at 25°C. The specific viscosity increment at infinite dilution was calculated for each polymer by extrapolation. In Table III, the symbol C is used to indicate that the concentration is expressed in volume fraction rather than in grams per liter. The density of the polymers was taken as 1.18 in making the conversion.

5. Discussion

The viscosity correction

The specific birefringence D has been defined by Eq. (2) with reference to the viscosity of the solvent. Signer and Gross[12] have reported that, for low molecular weight polystyrenes, the specific birefringence does not remain constant even in the most dilute solutions studied, unless it is referred to the viscosity of the solution. Mehl[14] discusses this point in connection with the double refraction of flow of tobacco mosaic virus protein. His own data are not extensive enough to permit a choice between the viscosity of solvent and solution in calculating D. In reviewing the experiments of von Muralt and Edsall on muscle globulin, however, he finds that the viscosity of the solution gives the more constant values for D. Since the equations involved in the theory of double refraction of flow and of the rotary diffusion constant refer to the viscosity of the solvent, empirical relationships involving the viscosity of the solution are difficult to interpret. It is probable that the correction can be avoided by working at lower concentrations.

Figure 1 shows that for dioxane solutions of methyl methacrylate polymers, D is constant and independent of the viscosity of the solution over a considerable range of molecular sizes. The failure of Signer and Gross to obtain a similar result may be attributed largely to their neglect of the birefringence of the solvent, cyclohexanone. Recalculation of their data for two polystyrenes of molecular weight 30,000 and 80,000 indicates that curves of the type shown in Fig. 1 may be obtained for these macromolecules. In the case of the muscle globulin experiments, it is quite possible that the concentrations used, 3 grams per liter to 15 grams per liter, belong in the region where D varies with concentration. The variation of ψ with concentration found in these experiments indicates that such is actually the case.

The relationship between D and θ_0

In Fig. 2, the reciprocal of the rotary diffusion constant, reduced to unit viscosity, is plotted as a function of the specific birefringence. The points, except for that given by polymer C fall fairly well on a straight line. The data can be compared with the requirements of the theoretical equations (5) and (7). Equation (5) de-

TABLE II. *Vortical angles of dioxane solutions of methyl methacrylate polymers. (Corresponding values of G/θ are given in italics.)*

	Gradient (sec.$^{-1}$)					
Polymer	4150	6200	8300	10,300	12,500	15,500
A					37.0	35.0
	—	—	—	—	*1.15*	*1.50*
B				31.5	28.0	26.5
	—	—	—	*2.15*	*2.90*	*3.30*
C					34.0	30.5
	—	—	—	—	*1.70*	*2.35*
D		29.5	23.0	25.0	22.5	17.0
	—	*2.55*	*4.50*	*3.80*	*4.75*	*7.95*
E	25.4	20.6	22.5	20.7	17.0	
	3.70	*5.75*	*4.75*	*5.75*	*7.95*	—

mands that the data fall on a straight line which passes through the origin. The relationship of Eq. (7) is not so obvious. Sadron has shown that for the polystyrenes, Δ'_c increases with molecular weight. Assuming this to hold true for methyl methacrylate polymers, and remembering that θ_0 decreases with increasing molecular weight, one sees that the variation in D due to the term in $1/\theta_0$ is of higher order than the variation due to $\Delta'/\theta_0\Delta'_c$. Hence, Eq. (7) may be written in the form,

$$D=k_1[1/\theta_0-k_2], \qquad (9)$$

where k_1 is a positive empirical constant, and where the positive quantity, $k_2=\Delta'/\theta_0\Delta'_c$, is assumed as a first approximation to be constant. The curve of Fig. 2 is consistent with the requirements of Eq. (9).

While the data for the vortical angle are probably not accurate enough to distinguish between Eqs. (5) and (7), the latter has a more sound theoretical basis, and the rotary diffusion constant will be considered to obey the approximate law of Eq. (9). On this assumption one may refer the rotary diffusion constants of the five polymers to their specific birefringences, rather than to the less accurately measurable vortical angles. Values of θ_0, corrected on this basis, are given in Table III.

Mass, shape, and structure of the methyl methacrylate polymers

From *a priori* considerations of the structure of methyl methacrylate polymers, one might predict that the macromolecule will behave as a rigid rod in solution. If one assumes the structure

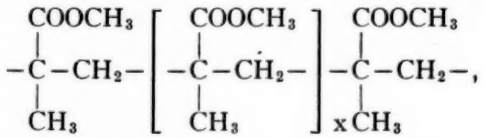

TABLE III. *Birefringence and molecular shape data for methyl methacrylate polymers (25°).*

POLYMER	$D\times10^{10}$	θ_0 OBS.	θ_0* CORR.	s (A)	M	s/d (AXIAL RATIO)	η_{sp}/C $(C\to0)$
A	0.09	127	149	890	34,000	89	75
B	0.29	55	64	1,170	45,000	117	210
C	0.42	84	48	1,300	50,000	130	270
D	0.69	27.5	32	1,500	58,000	150	410
E	1.32	17.5	18	1,880	72,000	188	640

* Rotary diffusion constants are measured in radians per second at unit viscosity.

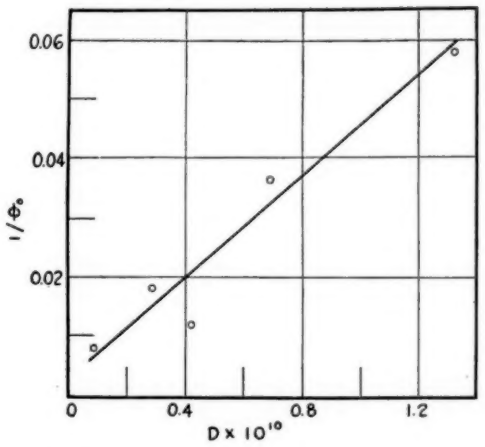

FIG. 2. Reciprocal of rotary diffusion constant as a function of specific birefringence for polymers A, B, C, D and E (cf. Table III).

then the strongly polar ester groups occur on alternate carbon atoms. At such a small distance, the repulsion between ester groups will be great, and will minimize any tendency towards "kinking," or rotation about the carbon-carbon bonds in the chain. This structure may be contrasted with that of ω-hydroxydecanoic acid polyester, in which a chain of nine single bond carbon to carbon linkages separates each polar group.

A Fischer-Hirschfelder molecular model of polymethyl methacrylate was constructed to correspond with the above structure. From an inspection of this model it was concluded that the macromolecule acts as a rigid rod, since there is little opportunity for kinking in the model.

Since Eq. (4) applies specifically to a long, rigid macromolecule, it can be used to calculate the lengths of the five polymers from their rotary diffusion constants. The corrected values of the latter were used in the calculation. The results are given in Table III.

The molecular model indicates that the polymethyl methacrylate macromolecule has a mean diameter of 10A. This will depend upon the particular structure assigned to the "backbone" carbon chain of the polymer. In our model, this chain consisted of a single row of carbon atoms. A chain consisting of a double row of carbon atoms is also sterically permissible, and this model would indicate a larger diameter. The values of the ratio of length to width s/d are listed in Table III for $d=10$A.

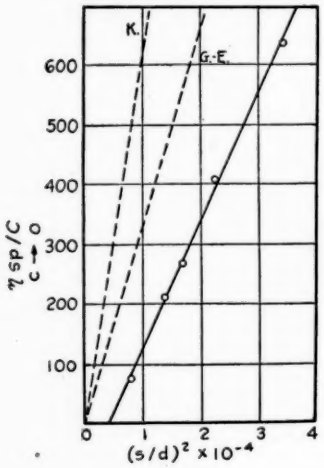

FIG. 3. Specific viscosity increment at infinite dilution for dioxane solutions of methyl methacrylate polymers as a function of the square of their length to width ratios. Dotted lines are theoretical—K., Kuhn; G.-E., Guth-Eisenschitz.

One may calculate the molecular weights of the polymers on the basis of a single row "backbone" chain by multiplying the values of s from Table III by 100/2.6, where 100 is the molecular weight of the monomeric unit and 2.6A is the length which the unit occupies in the chain. The molecular weights so calculated, also given in Table III, are minimum values, and again they depend upon the structure assumed for the carbon chain. The relative values of the molecular weight should be, of course, independent of this assumption.

Correlation with the specific viscosity increment

In Fig. 3 are plotted the specific viscosity increments, η_{sp}/C (extrapolated to infinite dilution) as a function of the square of the length to width ratio of the polymers. The dotted lines are obtained from theoretical equations (Kuhn, Guth-Eisenschitz). The dependence of the specific viscosity increment on the square of the length to width ratio is well substantiated. The slope of the experimental line is sensitive to the value assumed for the diameter of the macromolecule. If $d=10$A as assumed, the slope does not differ greatly from that demanded by the Guth-Eisenschitz equation. If d is assumed to be 16A, the slope corresponds to that given by the Kuhn equation. The most important discrepancy between theory and experiment is that the experimental line does not pass through the origin. The reason for this disagreement is not clear, although it is possible the failure to extrapolate specific viscosities to zero shear is involved. During the course of the experimental work it was assumed the flow is Newtonian because of the low concentrations of the solutions and the low gradients used.

Spontaneous orientation

It was pointed out in the previous section that the specific birefringence of the methyl methacrylate polymer solutions increases after a region of higher concentration is reached. On the basis of the orientation theory, this increase may be interpreted as being due to the action of orienting forces within the solution which are negligible at low concentrations, but which become operative when the solute concentration is increased.

The exact nature of these forces which produce spontaneous orientation is not definitely known. They may consist partly of long range van der Waals forces of the type described by London.[18] The macromolecules may tend to orient simply because this configuration corresponds to a minimum volume, and hence to a minimum energy for the system. The latter effect should disappear at low concentrations where no close packing is involved.

The data obtained for methyl methacrylate polymers may give positive correlation between a concentration at which spontaneous orientation sets in and the size of the molecule. If it is not unreasonable to interpret the data as has been done in Fig. 1, where all the curves turn upwards at the same value of S, the critical concentration is approximately proportional to the rotary diffusion constant, or to the inverse cube of the molecular length.

ACKNOWLEDGMENTS

This problem was suggested by J. W. Williams, and he has devoted much time and attention to its study.

The apparatus was constructed by Dr. O. T. Quimby.

The monomeric α-methyl methacrylate was supplied by the Roehm and Haas Company of Philadelphia, Pennsylvania.

The Wisconsin Alumni Research Foundation supplied fellowship assistance.

[18] London, Trans. Faraday Soc. **33**, 8 (1937).

Letters to the Editor

THIS section will accept reports of new work, provided these are terse and contain few figures, and especially few halftone cuts. The Editorial Board will not hold itself responsible for opinions expressed by the correspondents. Contributions to this section should not exceed 600 words in length and must reach the office of the Managing Editor not later than the 15th of the month preceding that of the issue in which the letter is to appear. No proof will be sent to the authors. The usual publication charge ($3.00 per page) will not be made and no reprints will be furnished free.

The Exchange Reaction between Gaseous and Combined Nitrogen

GEORGES G. JORIS
Frick Chemical Laboratory, Princeton University, Princeton, New Jersey
September 9, 1941

THE exchange reaction between gaseous and combined nitrogen recently reported in a letter to this journal by Yoshio Nishina, Takeo Iimori, Hideo Kubo and Hiromi Nakayama[1] has been reinvestigated using stable heavy nitrogen isotopes N^{30}_2 and N^{29}_2. The composition of the initial gaseous mixture was $N^{28}_2 : N^{29}_2 : N^{30}_2$, 1000 : 204 : 100. Aqueous solutions of $NaNO_2$, $NaNO_3$ and $NH_2OH \cdot HCl$ at a concentration of 1/20 mole/l were used since they were reported to undergo the most rapid exchange between gaseous nitrogen and combined nitrogen.

No exchange was found as shown by the ratios N^{29}_2/N^{30}_2 with the shaking time indicated in Table I.

TABLE I.

SUBSTANCE TESTED	0 HOUR	6 HOURS	30 HOURS	360 HOURS
$NaNO_3$	2.04	2.05	2.05	2.04
$NaNO_2$	2.04	2.05	2.04	2.05
$NH_2OH \cdot HCl$	2.04	2.03	2.05	2.03

The results recorded with radioactive nitrogen must therefore be ascribed to difficulties arising in the technique of operation with the radioactive isotope. The present results are more reasonable, judged from the chemical standpoint and the stability of the ions containing nitrogen.

[1] Y. Nishina, T. Iimori, H. Kubo and H. Nakayama, J. Chem. Phys. 9, 571 (1941).

The Infra-Red Absorption and Reflection Spectra of KHF_2 and of KDF_2

J. A. A. KETELAAR
Laboratory for Inorganic and Physical Chemistry, University, Leyden, The Netherlands
September 5, 1941

THESE compounds were investigated with a prism spectrometer in the quartz and rocksalt regions from 1–16μ. When the investigation of ordinary potassium bifluoride was about finished a note came to my knowledge from Messrs. Buswell, Maycock and Rodebush.[1] These authors only investigated the quartz region and here our results are in complete accordance. However my much more extensive investigations have led to conclusions essentially different from theirs.

The maxima at 1222 cm^{-1} and 1450 cm^{-1} (in reflection 1238, 1490 cm^{-1}) are both fundamental bands as indicated by the extreme strong absorption (> 90 percent for a layer of 8μ) and by the high reflection percentages (55 percent and 60 percent, respectively) for both bands, thus excluding the explanation as a combination frequency for the latter band. The three other pairs of bands of decreasing intensity below 3500 cm^{-1} are due to combination frequencies of these fundamentals with 1, 2, and 3 times a frequency of 560–600 cm^{-1}. Of these pairs also the higher frequency component is the strongest band. The bands above this limit are due to the second harmonics[2] of the fundamentals at 3730 cm^{-1} (double) and at 5099 cm^{-1}, respectively, and

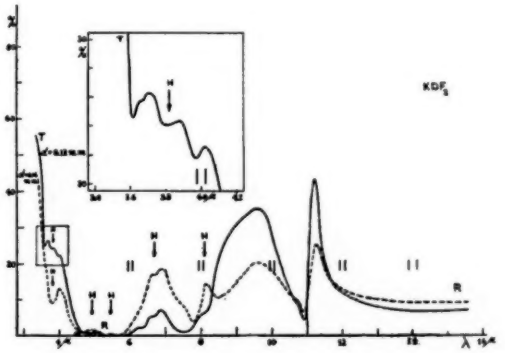

FIG. 1. Transmission and reflection curves for KHF_2 in the rocksalt region.

to their combinations with the same frequency of 560 cm^{-1}. The doubling of the band at 3730 cm^{-1}, also observed by the other authors, is due to a minor complication, the splitting of an higher harmonic due to higher terms in the potential function. The spectrum of KDF_2 is explained in just the same way with a shift of the fundamental bands by about $\frac{1}{2}\sqrt{2}$ to 891 cm^{-1} and 1046 cm^{-1} (in reflection). The inactive frequency at 560 cm^{-1} is found to be independent of the mass of the hydrogen atom. Thus a complete analysis of all bands in both spectra is possible with a single exception of minor importance.

The spectrum observed is due to the isolated HF_2 group as indicated by the identity between the spectra of KHF_2 and $RbHF_2$, save for a shift of a few cm^{-1} to lower values for the latter compound. Moreover specimens of KDF_2 containing 10 percent H give a mere superposition without any shift of the spectra of the pure compounds, thus proving the absence of any appreciable coupling between the groups. The fundamental double band is to be associated with the asymmetric valency oscillation of a linear three atomic model ("hydrogen frequency"), whereas the frequency at 560 cm^{-1} is the symmetric one ("fluorine fre-

quency"). The doubling of the active frequency can be shown to be only due to the existence of a double minimum in the potential curve for the hydrogen atom. A potential curve constructed according to the method of Dennison and Uhlenbeck[3] from the experimental data gives 2570 cm^{-1} for the height of the potential hump with a separation of both levels of 25 cm^{-1} and 185 cm^{-1} for the ground and for the first excited level, respectively, the latter being already very near the top of the hill. The distance between both minima is found as only 0.70 angstrom units.

These results prove for the first time the existence of protonic resonance in the case of a hydrogen bond. On the other hand the small doubling of the ground level proves definitely that even here this resonance does not contribute to any extent to the energy of the bond formation ($\frac{1}{2}h\nu$ = 0.04 kcal./mole) which consequently must be considered to be entirely of electrostatic origin, due to the partial ionic character of the hydrogen atom. The structure of the HF_2 group is thus symmetric, resonating between F HF and FH F.

Experimental details are given in a forthcoming publication in the Rec. trav. chim.

[1] A. M. Buswell, R. L. Maycock and W. H. Rodebush, J. Chem. Phys. **8**, 362 (1940).
[2] The first harmonics are absent due to a selection rule valid for the crystal.
[3] D. M. Dennison and G. E. Uhlenbeck, Phys. Rev. **41**, 313 (1932).